COMPARATIVE STUDY OF BISTATIC INTERSYSTEM INTERFERENCE IN TROPICAL LOCATIONS

OJO, JOSEPH SUNDAY
(PHY/92/4138)

A THESIS SUBMITTED IN PARTIAL FULFILLMENT OF THE REQUIREMENTS FOR THE AWARD OF THE DEGREE OF

MASTER OF TECHNOLOGY (M.TECH)

IN

COMMUNICATION PHYSICS

DEPARTMENT OF PHYSICS

FEDERAL UNIVERSITY OF TECHNOLOGY,
AKURE, NIGERIA

DECEMBER 2003

CERTIFICATION

I certify that Mr. J.S. OJO has carried out this work under my supervision in the department of physics, Federal University of Technology, Akure, Ondo State, Nigeria.

M.O Ajewole. B.Sc. M.Sc. (Ilorin) Ph.D (Akure)
Department of physics
Federal University of Technology
Akure, Nigeria.

December 2003

DEDICATION

This work is dedicated to the glory of Almighty God.

TABLE OF CONTENTS

LIST OF FIGURES

LIST OF TABLES

ABSTRACT

Very many prediction models have been used in recent times to estimate transmission loss arising from bistatic scattering of terrestrial microwave signals into the receiver of Earth-space communication systems operating at the same frequency. Among the models, the Capsoni simplified 3-D EXponential rain CELL (EXCELL) model has yielded the most satisfactory results for interference prediction in all rainfall climate regions. In the model, the horizontal structure of rain is the same in all regions, hence only the measured cumulative distribution of point rainfall rates in the region of interest is required. This study is based on this model. It uses as input measured cumulative distribution of rainfall rates from three locations in Africa, Ile-Ife (Nigeria), Nairobi (Kenya) and Douala (Cameroon) to estimate bistatic intersystem interference (transmission loss) due to hydrometeor scattering of signals from a terrestrial microwave system into the receiving terminal of a ground Earth-space communication system. Two elevation angles, 23^0 and 55^0, which are the prominent satellite look angles in Nigeria are considered. The transmission loss statistics are computed for varying distances from the Terrestrial System (TS) antenna to the Common Volume (CV) formed by the intersection of the antenna beams, varying antenna gains and varying percentage unavailabities. Frequencies ranging from 4 to 35 GHz and two path length configurations short (≤ 50 km) and long (> 50 km) are considered. Results obtained show that transmission loss increases with increasing TS to CV distance, implying decreasing probability of severe interference in the satellite system. The variation of transmission loss with increasing TS antenna gain shows that transmission loss increases with decreasing time unavailability (exceedance probability). The study also shows that for a given fade depth, transmission loss decreases linearly with increasing TS antenna gain. Therefore, for a given fade depth, the higher the TS antenna gain, the higher is the probability of the ground satellite receiver

picking severe interference from the terrestrial microwave network. Further, comparing the results in Kenya and Cameroon with Nigeria, it was observed that variation of transmission loss with TS to CV distance is lower by 1.3% in Kenya, while it is higher by 1.4% in Cameroon for 0.01% time unavailability. Therefore, in Cameroon, the satellite ground receiver system is more likely to receive higher interference from a microwave transmitting system operating at the same frequency. Evaluation of the effective transmission loss in these regions also show the possibility of complete signal outage due to rain attenuation in Cameroon compared to other locations, no matter the amount of interference received from the microwave system. This is because of the higher rainfall intensity and accumulated water in Cameroon.

CHAPTER ONE

1.0 Introduction

The advent of the communication satellites and other technologies like the Very Small Aperture Terminals (VSATs) for wireless internet browsing, Digital Visual Display (DVD) and sound broadcast services among others as part of the integrated radio communication and information networks has increased the need for more efficient use of the spectrum.

As a result, techniques such as frequency re-use where a terrestrial radio relay link will use the same frequency as the earth station link have been employed. Such shared facilities may experience interference and one such mode is bistatic hydrometeor interference. It is therefore necessary, to be able to estimate the effects of propagation and scattering across a wide range of frequencies.

The interference that occurs for several geometries (different antenna bearing) is due to the omni-directional nature of the precipitation scatter. This is so since the signals intended for the microwave system may be scattered by hydrometeor to cause interference in another microwave system operating at the same frequency (Thurai, 1994).

Hydrometeor is the general term referring to the products of condensed water vapor in the atmosphere usually observed as rain, hail, ice, fog, cloud or snow. The most important and widespread of these hydrometeors to radio propagation is rain. An electromagnetic wave propagating through a region containing raindrops suffer two attenuating mechanisms; part of its energy is absorbed by raindrops and transformed to heat (absorption), while another part is scattered in all directions -scattering (Medeiros Filho et al., 1986).

The bistatic hydrometeor interference is due to intersection of a terrestrial beam and an earth station beam. The interference will result in the decrease of the signal to noise ratio at the interfered terminal, and, it can lead, in the worst case, to link outage depending on the severity of

the received interference levels. Viewing the extent of such interference on statistical terms is highly important for the service planners and designers so as to be able to assess the degree of coupling between the systems.

Also, the presence of precipitation particles in the volume formed by the intersection of the transmitting and receiving antenna beams of two independent communication systems operating at the same microwave frequency may result in scattering and bistatic interference. This is because part of the electromagnetic energy propagating along a given direction can be scattered in the receiver's direction and cause harmful interference. The level of such interference is dependent on the specific geometry, the characteristics of the two antenna systems and the structure of rain in the medium.

For the prediction of interference, the following parameters are needed to calculate the transmission loss due to hydrometeor scatter between two microwave stations. These parameters are: electrical, system, meteorological e.t.c. A lot of models backed with experimental validations have been proposed and tested using data from the temperate region. In the tropical regions including tropical Africa, the problem of interference due to rain scattering is just receiving attention, and that explains much of the problems associated with the use of microwave communication systems in this region. Notwithstanding the above, quite modest contributions have been made in Africa, by the work of Ajewole et al., (1999) and the most recently by Ajewole, (2003).

In tropical climates, convective rainfall activity is far more prevalent where strong vertical air motions give rise to large scale mixing of frozen liquid and partially melted hydrometeors. Convective rainfall also results in the super cooled drops or wet hail being present at large height giving rise to high values of reflectivity (Thurai, 1994). Many models have been proposed for the prediction of interference due to hydrometeors. Among these models, the ones based on the

assumption of an exponential rain cell model, Capsoni et al., (1987), Capsoni and D'Amico, (1997) and Awaka, (1989) are quite unique. This is because they assume that the horizontal structure of rain is the same in all rainfall zones (Ajewole, 2003). Due to the enormity of computation required in using the complete version of the model, Capsoni et al., (1992) proposed the simplified version of the 3-D method of predicting cumulative distribution of transmission loss and this is utilized in this study. In the exponential rain cell model for predicting interference, the metrological environment is modeled through a population of synthetic rain cells whose characteristics have been deduced from studies on the horizontal structure of precipitation carried out on rain maps as reported in Cost project (Cost 210). The limitations of the model include; yielding excessively large rain cell radius when rain intensity is $\leq 6 mmh^{-1}$ and overestimating the attenuation of the wanted signal in the computation of the effective transmission loss. Hence, it is suited for the prediction of intersystem interference due to convective rainfall.

1.1 The Scope of the study

In this report, investigation of hydrometeor scatter as one of the propagation factors that can affect the availability of wanted signal in a tropical environment is investigated. Emphasis is on the availability of satellite channels receiving interfering signals from a low elevation angle $\sim 1^0$, terrestrial microwave relay link operating at the same frequency as a result of hydrometeor scatter in the common volume formed by the terrestrial station. The study is limited to the frequency range 4 – 35GHz where there is high degree of frequency sharing and coordination between the terrestrial and Earth-space systems. The terrestrial antenna gain varies from 35 –55dB and for practical consideration, the probability of occurrence levels ranges from about $1\text{-}10^{-5}\%$. The mean annual statistics of the cumulative distribution of point rain rate P (R) measured at the locations (Ile –Ife, Nigeria, Douala, Cameroon and Nairobi, Kenya) are used. Convective thunderstorm rain

type is assumed, since this rain type is prevalent in the three locations. The interfering signals are assume to be vertically polarized

CHAPTER TWO

2.0 THEORETICAL BACKGROUND

Consider an electromagnetic energy radiated by a transmitting antenna and assume that this illuminates a region of space, which is intercepted by atmospheric precipitation. Using this same region to view the antenna beam of a receiving terminal operating at the same microwave frequency, interference may occur. The scattered wave arriving at the receiving antenna is composed of a very large number of elementary waves. Each elementary wave is generated from a single hydrometeor in the common volume and assuming that each elementary wave is different from the others in size, shape, location and movement. In addition, all these elementary waves have undergone attenuation while traveling on slightly differing paths.

Fig 2.1 is a sketch of typical 'hydrometeor scatter' propagation geometry from a terrestrial system to an Earth – space system. The path geometry of hydrometeor scatter interference is usually defined in terms of the station separation, their projection to the common volume and also their relative bearing. Table 2.1 shows these variables, their corresponding common volume heights and the horizontal extents as are applicable to the present study.

Let us consider the presence of scatterers in the common volume, that is, the region of space defined by the intersection of the two antenna beams, from fig 2.1, part of the energy propagating along r_1 is redirected along r_2

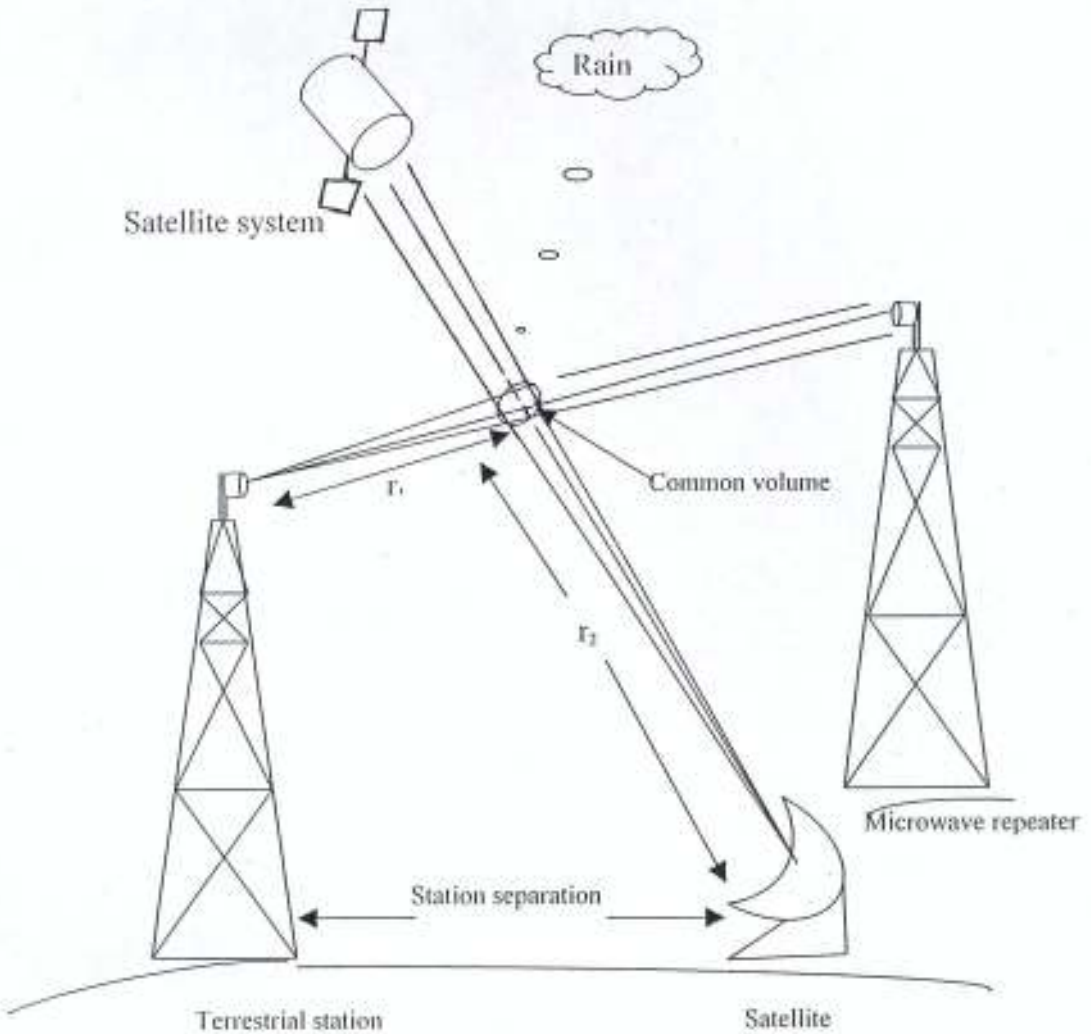

Fig.2.1 Hydrometeor scatters propagation geometry from a terrestrial system to an Earth-space system operating at the same frequency.

Table 2.1 some geometrical parameters for calculating transmission loss.

r_1 (km)	Station Separation (km)	r_2 (km)	CV height (km)	CV length (km)
50.0	50.7	1.245	0.711	1.021
100.0	101.6	2.849	1.620	2.343
150.0	152.7	4.810	2.725	3.966
200.0	204.0	7.135	4.022	5.893
250.0	255.4	9.812	5.507	8.121

CV- Common Volume

2.1 THE BISTATIC RADAR EQUATION (BRE)

The amount of (unwanted) energy that reaches the Earth – space system (receiver) can be evaluated through the Bistatic Radar Equation developed by Crane, (1974) in terms of the ratio of signal power in the two systems. Neglecting multiple scattering by atmospheric particle, BRE can be expressed as

$$\frac{P_r}{P_t} = G_t(i)G_r(0)\frac{\lambda^2}{(4\pi)^3}\int_v \frac{F_t(\vartheta_1,\phi_1)F_r(\vartheta_2,\phi_2)A_t(r_1)A_r(r_2)A_g}{r_1^2 r_2^2}dv\int_0^\infty N(D)\sigma_s(i,\alpha,D)dD \qquad (2.1)$$

where P_t and P_r are respectively the mean power (in watts) transmitted and received along the axis of the main antenna beams, $F_{t,r}(\vartheta,\phi)$ represents the directivity function of the antenna systems from which the effective areas are calculated. $A_{t,r}(r_{1,2})$ represents the attenuation along the paths from and towards the elementary volume, while Ag is the attenuation due to gaseous absorption. $G_{t,r}$ are the transmitter and receiver antenna gains, while λ is the wavelength of the radio signal, r_1 and r_2 are the path length from the transmitter to the common volume, and from the common volume to the receiver, D is the particle equivolumic diameter, N (D) is the particle number density in a diameter interval dD, σ_s is the total scattering cross- section of particles with diameter D inside the common volume, and it is related to the reflectivity factor, point rain rate R, and the complex refractive index of the raindrops. At frequencies above 10GHz, and as raindrops size gets bigger than 3mm correction for Rayleigh scattering must be taken into consideration.

To calculate the transmission loss, L or interference levels, the inverse log of equation (2.1) will be taken, to yield

$$L = 10\,\mathrm{Log}_{10}\frac{P_t}{P_r} \qquad (2.2)$$

The evaluation of equation (2.2) depends on several factors such as the link geometry, electrical, and meteorological parameters and these are also interdependent, as such, it is very difficult to evaluate equation. (2.1) together once. From the physical point of view, extracting all the terms

from the integral in equation (2.1) implies that the common volume is reduced to a single point corresponding to the intersection of the two antenna axes where the total scattering cross section is evaluated. This is called the pencil beam approximation.

2.2 THE SIMPLIFIED BRE

The common volume is assumed to be very small compared to r_1 and r_2 in equation (2.1). A_t and A_r are assumed independent of their positions in the common volume, and the total scattering cross section is also assumed constant within the common volume thus, the common volume is much smaller than the rain region. Hence, the simplified form of the complete 3-D BRE is expressed as

$$\frac{P_r}{P_t} = \frac{A_t(r_1)A_r(r_2)A_g G_t(i)G_r(o)\lambda^2\sigma_{bi}}{(4\pi)^3 r_1^2 r_2^2} \times \int_v F_1(\vartheta_1,\phi_1)F_2(\vartheta_2,\phi_2)dv \qquad (2.3)$$

The symbols are as defined previously in equation (2.1), while σ_{bi} is the scattering cross section per unit volume of precipitation; it replaces the second integral term on the far right of equation (2.1). This quantity depends on the frequency and polarization of the incident and scattered waves and on the value of refractive index, size, and shape of the hydrometeor among others.

For interference simulations and predictions it is convenient to take into consideration the worst case, since the highest value of coupling occurs when the transmitted and received waves are both vertically polarized, whatever the scattering angle (Awaka and Oguchi, 1982). Hence spherical drops are chosen and vertical polarization is assumed. The scattering cross section of each single particle can then be evaluated numerically using the complete Mie solution or Rayleigh approximation. At frequencies less than 10GHz, the scattering cross section per unit volume of precipitation σ_{bi} is expressed as

$$\sigma_{bi} = (10^{-18})\frac{\pi^5}{\lambda^4}\left|\frac{\varepsilon-1}{\varepsilon+2}\right|^2 Z \qquad (2.4)$$

where λ is the wavelength in meters, ε is the permittivity of the medium (that is frequency, temperature, and particle phase dependent) and Z (mm^6m^{-3}) is the so called radar reflectivity which is proportional to the sixth power of the drop diameter, that is

$$Z = \int_0^\infty N(D)D^6 dD = \int_0^\infty N_o e^{-\Lambda D} D^6 dD \qquad (2.5)$$

where N (D) dD is the density of raindrops in a diameter interval dD, No=8000 ($m^{-3}mm^{-1}$) and $\Lambda=4.1R^{-0.21}$ (mm^{-1}) (Marshall and Palmer, 1948). The integration in equation (2.5) can be avoided by using a power law relation of the form

$$Z = a\,R^{b} \qquad (2.6a)$$

where R is the rainfall rate (mm/h). Then,

$$Z = 10 \log z \qquad (2.6b)$$

For tropical thunderstorm rain type assumed in this study, the parameters of 'a' and 'b' of equation (2.6a) are 'a' =464 and 'b' =1.31 respectively (Ajayi and Owolabi, 1987). For vertical polarization, the total scattering cross section is expressed as the ratio of the analogous quantity in the Rayleigh regime and a correcting factor S, that is,

$$\sigma(\hat{i}, \hat{o}) = \sigma_{bi}(\hat{i},\hat{o})/S \qquad (2.7)$$

where σ_{bi} is defined by (2.4) and

$$10 \log S = R^{0.4} 10^{-3}\left[4(f-10)^{1.6}\left(\frac{1+\cos\varphi s}{2}\right)+5(f-10)^{1.7}\left(\frac{1-\cos\varphi s}{2}\right)\right] \qquad (2.8)$$

Note that 10 log S=0, if f ≤ 10 GHz, where f is the frequency (GHz) and φ_s is the scattering angle. Using equation (2.6a) multiplied by the constant 'σ' in equation (2.4) and replacing the second integral on the far right of equation (2.1) by this new quantity, we are then left with the integral on the far right of equation (2.3) defined as the effective common volume V_w.

$$V_w = \int_v \frac{Fi(\vartheta_1,\varphi_1)Fr(\vartheta_2,\varphi_2)}{r_1^2 r_2^2} dv \qquad (2.9)$$

2.2.1 THE EFFECT OF SIMPLIFIED (BRE)

Using the simplified BRE of eqn. (2.3) leads to a dramatic reduction of computing time. The effective common volume must be evaluated once for a given geometry, regardless of the specific rain pattern. It implies that in order to compute a single interference level, only two-monodimensional integration are required for the calculation of the extra attenuation and total scattering cross section.

The scatter cross section has to be independent of the vectors $\hat{i}$ and $\hat{o}$, whatever the position of the particle in the common volume. Considering the beam pattern of the receiving antenna as being much narrower than the transmitting antenna, when the axes of the beam intersect each other, the transmitting pattern is almost constant within the common volume. The pencil beam widths are also reduced to straight lines while the common volume becomes a point, which will be the actual intersection point of the antenna axis (Capsoni. et al., 1992).

Taking the contribution from the elementary volume forming the common volume, equation (2.1) can further be simplified in terms of the transmission loss L, into

$$L = P_t - P_r = K_T + A_g - M + (S - Z + A) \qquad (2.10)$$

All the terms in equation (2.10) are in decibel (dB) units. P_t and P_r are the transmitted and received power, Ag is the extra attenuation due to gaseous absorption, M is the polarization decoupling factor, S is as defined in equation (2.8) and A is the slant path rain attenuation from the transmitter to the common volume and from the common volume to the satellite receiver. This is calculated using the power law relationship between rain rate and attenuation which is expressed as

$$A_v = k_v R^{\alpha_v} \qquad (2.11)$$

The subscript v refers to vertical polarization and the parameters k_v and α_v for calculating attenuation A are shown in Table (2.2) for the frequencies investigated in this study. Z, the radar

reflectivity has been defined in equation (2.6a) and (2.6b). The term K_T in equation (2.10) takes the form,

$$K_T = 10\log\left[\frac{G_1 G_2 \pi^2}{64^3 \lambda^4}\left|\frac{m^2-1}{m^2+1}\right| \times 10^{18} \int \frac{F_1(\vartheta_1,\varphi_1)F_2(\vartheta_2,\varphi_2)}{r_1^2 r_2^2} dv\right] \qquad (2.12)$$

where G_1 and G_2 are the antenna gains, m is the complex refractive index of water, λ is the wavelength of the wave, F_1 and F_2 are antenna directivity functions, r_1 and r_2 corresponds to the slant path length from the interfering terrestrial station and from the satellite station to the common volume respectively while dv is an elementary volume

Table 2.2.Regression parameters k and α of the power law expression for the thunderstorm rain type (from Ajewole, Kolawole and Ajayi, 1999). V represents vertical polarization states.

FREQUENCY (GHz)	k_v	α_v
4.0	6.32×10^{-4}	1.01970
6.0	2.61×10^{-3}	1.06560
8.0	7.36×10^{-3}	1.11700
10.0	0.01520	1.12970
12.0	0.02580	1.11200
16.0	0.05963	1.06851
20.0	0.83400	1.03000
34.8	0.25693	0.99030

2.3 INTERFERENCE DUE TO HYDROMETEOR MODELS

A lot of models and prediction techniques have been used for determining interference due to hydrometeor scatter between two independent microwave stations. Among the most widely used models are; International Radio Consultative Committee (CCIR) model of report 569(1990) as reported in Cost 210, International Telecommunication Union-Radio committee (ITU-R) model, Capsoni's model, Crane model, Awaka model, Gaussian profile model, and the simplified 3D cell model among others. Among the pack, the Capsoni exponential rain cell model is unique, because it demonstrated that the horizontal structure of rain is the same in all rainfall climatic zones. The difference among rainfall zones lies in the measured cumulative distribution of rainfall rate of the ITU-R. The present study employs the modified 3-D cell model of Capsoni in the computation. In what follows, some of the most widely used model are also described.

2.3.1 THE CCIR MODEL

The International Radio Consultative Committee hydrometeor scatter model is intended to predict transmission loss statistics from rainfall rate statistics. It is based on two fundamental assumptions: Scattering which occurs only within rain cells having circular cross section and whose diameter depends on the rainfall rates inside the cells, and Attenuation; which occurs inside as well as outside the cell, but only below the rain height. Statistics of measured data on the 11 – 18GHz range seems to show reasonable agreement with the predictions on the basis of the model (COST 210, Report 569, 1990). At higher frequencies (30GHz and above), however, larger deviations have been observed.

One other assumption is that of the time- invariant rain height, which determines whether the scattering occurs in the rain or in the ice region. The limitations of the model however are:

(i) Only coupling between a narrow – beam earth station and a distant terrestrial radio relay station is considered:

(ii) exact intersection of antenna axes is assumed, while the side-lobe coupling is not considered;

(iii) no side scatter is included in the analysis only forward and back scatter are considered.

The CCIR model was later modified and the resulting expression for the determination of transmission loss at frequency f, is

$$L = 168+20 \log r - 20 \log f - 13.2 \log R - g_T + 10\log A_b - \log C + \Gamma + \gamma_0 d_0 + \gamma_v d_v \quad (2.13)$$

where r is the distance between the region of maximum scattering and the location of an earth station, R is the surface rainfall rate (mm h^{-1}) for the required climatic region; g_T is the gain of the terrestrial station antenna, A_b is a correction factor for non- Rayleigh scattering, C is the effective scatter transfer, and is expressed as

$$C = \frac{2.17}{\gamma_R d_s}\left(1 - 10^{-\gamma_R d_s / 5}\right) \qquad f > 4GHz \qquad (2.14a)$$

$$1 \qquad f \leq 4GHz \qquad (2.14b)$$

$$\gamma_R = kR^{\alpha} \qquad (2.15)$$

$\gamma_0 d_0 + \gamma_v d_v$ are the atmospheric attenuation for Oxygen and water vapor respectively.

$$d_s = 3.5\, R^{-0.08} \qquad Km \qquad (2.16)$$

$$\Gamma = 631\, k\, R^{\alpha-0.5} \cdot 10^{-(\theta+1)^{1.5}} \qquad dB \qquad (2.17)$$

2.3.2 Gaussian profile model.

It uses non- orthogonal gaussian function expansion of vertical reflectivity profiles. In addition, it allows quick calculation of the bistatic radar cross-sections in hydrometeor scatter problems involving arbitrary reflectivity profiles. In particular, it allows scattering from melting band and ice regions to be included in the cross –section calculation. This model however lacks a physical basis.

2.3.3. The Crane model

Crane, (1974) investigated the bistatic scatter from rain using weather radar instrument in the Avon – to- Westford (Country). He was the first to undertake detailed measurement of the effect, and his work remained for a long time the basis of the ITU-R prediction method (Ajewole et al., 1999). Transmission loss was estimated for the bistatic scatter paths, which were computed using the weather radar data, the bistatic radar equation, and a model for the scattering cross section per unit volume of rain based upon Rayleigh scattering by an ensemble of water sphere. The model predicts low values of rain cell size for all rain conditions.

2.3.4 The ITU-R Model

This model predicts the distribution of rainfall rate in a locality. It investigates the problem of hydrometeor interference by assuming the 3-D exponential rain cell model of Capsoni et al., (1997). The model offers possibility of predicting the statistics of many propagation parameters such as attenuation, interference by rain scattering etc, which are determined by the rain cell characteristics, and their frequency of occurrence. The model has some limitations such as; yielding excessively large rain cell radius when rain intensity is less or equal to $6mmh^{-1}$, overestimating the attenuation of the wanted signal in the computation of the effective transmission loss. Also, the non-inclusion of the relationship between the reflectivity factor and the attenuation on one hand, and the assumption of a fixed rain cell position in space is another limitation of the model.

2.4 The 3D CELL Model

Due to the limitations associated with models described earlier, a three-dimensional rain cell model (3-D cell model) has been developed to examine a non-fixed cell situation and to improve on the aforementioned limitations.

Hydrometeor scattering is observed when a rain cell passes through the common volume, which is defined by the intersection of the antenna main beams. At any given time, the transmission loss can be computed by the BRE if the location and structure of the rain cell are specified. The computed transmission loss may vary with time because of the movement of the rain cell and because of the temporal change in the rain cell structure. For simplicity, this study assumes that the rain cell structure does not change in time. Then the temporal changes in the transmission loss occur only because of the movement of the rain cell. Hydrometeor scattering is observed when a rain cell overlaps with the common volume. After the rain cell moves away from the common volume, no hydrometeor scattering is observed for a while. Then there comes another rain cell with different size and intensity into the region of common volume, and hydrometeor scattering resumes. When this process continues for a long time, all possible values of the transmission loss are obtained. The ergodic hypothesis Mismie and Waldteufel, (1980) enables us to compute the probability of observing the values of transmission loss. Hence, the cumulative distribution of the transmission loss can be computed.

The procedure above requires specifications of the rain cell structure and the movement of the rain cell.

2.4.1 Rain – cell structure (Spatial structure of rain cell)

The spatial structure of precipitation rate (mm h^{-1}) in both the vertical and horizontal direction is needed to compute statistics of transmission loss. The vertical structure of precipitation assumes that rainfall rate is vertically homogeneous up to the effective rain height. As a matter of fact, the

structure of precipitation is assumed constant up to the 0°C isotherm height, below which is the rain region where attenuation and scattering of the wanted and the interfering signals occur. Beyond the 0°C, is the ice region where Z decreases at the rate of 6.5dB/Km, hence, attenuation is small (Ajewole, 2003). Z is climate/region dependent. It varies in the temperate region, while it is relatively stable in the tropical climates (Ajayi and Barbaliscia, 1990). The physical rain height on the other hand is a more practical quality for defining the height of the rain region especially for rainy conditions. The expression proposed by the ITU-R for the mean 0°C isotherm height (h_0), which can be equated to the mean 0°C isotherm height (h_{FR}) during rain conditions in the tropical region is

$$h_{FR} = 5.0 \text{ Km} \quad 0 < \phi \leq 23 \tag{2.18a}$$

ϕ is the latitude of the locations. Due to the over-estimation of the h_{FR} by this model worldwide, Ajayi and Babaliscia (1990) used radiosonde data to propose a relationship for h_{FR} for Nigeria. This relationship depends weakly on the rain rate value averaged over a 2hr period, 1hr before and 1hr after the launch of the radiosonde. It is expressed as

$$h_{FR} = 4.67 + 6x10^{-3}R \tag{2.18b}$$

An example of the horizontal cross section of a rain cell is shown in figure (2.2). The rain cell has a cylindrical symmetry. Within the horizontal cross section, the rainfall rate is assumed to vary exponentially at point x and y and is expressed as

$$R(x, y) = R_m e^{-r/r_0} \tag{2.19}$$

where r is the radial distance with coordinate (x, y) from the rain cell center, R_m is the maximum rainfall rate and r_0 is the parameter characterizing the cell size. (Capsoni et al., 1987)

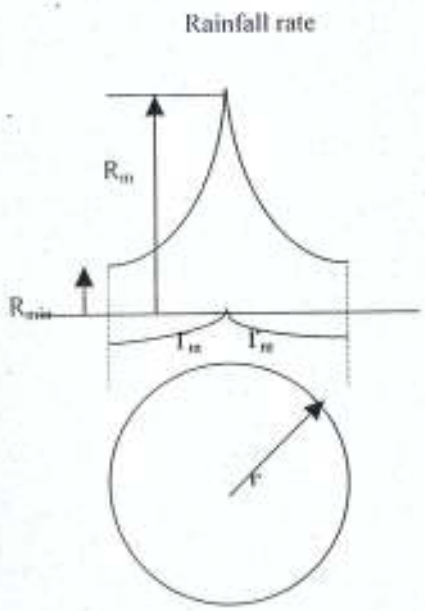

Fig.2.2 Horizontal cross section of a rain cell

It is necessary to truncate r at a certain distance r_m where the rain intensity is minimum (R_{min}). R_{min} occurs at the distance at which $r = r_o$ and there is no rain when r is greater than r_m.The expression can be written as

$$r_o = \frac{r_m}{\ln \frac{R_m}{R_{min}}} \tag{2.20}$$

According to Capsoni and D'Amico (1997), for any range of peak rain rate, rain cells present well- defined exponential distribution of sizes regardless of the range of R_m considered. A probability density is then attached to this exponential distribution, which is a function of the conditional average radius (size) of the rain cells. This conditional average radius (size) is expressed as

$$r_o(R_m) = 1.7\left[\left(\frac{R_M}{6}\right)^{-10} + \left(\frac{R_M}{6}\right)^{-0.26}\right] \tag{2.21}$$

2.4.2 Rain – cell movement

Rain cells are assumed to have constant velocity. Let us consider identical rain cells in the first place. Though the cells are identical in structure, the closest distance between the center of the cell and the center of the common volume, which is a similar concept to the impact parameter in the collision theory, varies with each cell. This closest distance is assumed distributed uniformly in statistical senses.

In actual fact, the center of the common volume is located at a fixed point whereas the rain cells move about. However, since the rain cells are assumed to be identical and are also assumed to have the same velocity, the actual situation can be regarded as equivalent to the following situation in a statistical sense: A rain cell is fixed in space whereas the center of the common volume moves about uniformly on a horizontal plane in the rain cell.

We also assume that each type of rain cell contains infinite number of identical cells crossing the common volume. Values of the transmission loss vary depending on the position of the center of the common volume in the rain cell. The above statistically identical situation enables us to compute the cumulative distribution of transmission loss.

2.4.3 The spatial density

The exponential shape, the type of distribution of rain cell sizes, and the conditional average radius are valid in any location. Hence, any meteorological rain environment can be modeled by a group of isolated rain cells having different peak rain rates and sizes by attaching an appropriate statistical weight. This fact enables us to utilize the Excel shape model of the horizontal structure of rain. The difference from one location to another is reflected in the probability of occurrence of a rain cell which is represented by the cell spatial density; that is the number of cells per square kilometer and per unit peak rain rate, R_m and r_o. It is expressed as

$$N(r_o, R_m) = N^*(R_m)\exp\left(\frac{-r}{r_o(R_m)}\right) \tag{2.22}$$

where $N^*(R_m)$ is the spatial density of cells with peak rain rate R_m no matter the value of r_o. This parameter is related to the cumulative distribution of the point rain rate, which is location dependent, and is easily available from the measurement at the location of interest or from ITU-R rain climatic zones.

In relation to area probability, Capsoni et al., (1987), further simplified $N^*(R_m)$ by setting the probability P (R) of finding R (x, y) of equation (2.19) greater than R', and proportional to the geometric area over which R is greater than R', thus for a third order derivative of R_m,

$$N^*(R_m) = \frac{-1}{4\pi R_m r_o(R_m)}\left|\frac{d^3P(R)}{d(\ln R)^3}\right|_{R=Rm} \tag{2.23}$$

A log- power –law expression was then adopted to define the measured values of P (R). The expression proposed is given as

$$P(R) = P_o \ln\left(\frac{R'}{R}\right)^k \qquad (2.24)$$

P_o and k can be obtained by interpolation from cumulative distribution of the measured point rain rate P (R) or from the ITU-R (1999) rain climatic zones. R' is normally assumed to be about four times the highest rain rate at the location of interest. The summary of P_o, R^* and k for the three locations, Nigeria, Kenya and Cameroon is shown in Table 2.3. An average water vapour density of $20g/m^3$ was assumed to calculate attenuation due to absorption by atmospheric gases (ITU-R Rec.P.836-1, 1997) while water temperature of 20°C was assumed to calculate refractive index of water using the method of Ray, (1972).

Table2.3 Power law parameters for the local cumulative probability density for thunderstorm convective rain type for the locations considered and the Z – R relation.

Location	P_o	R^*	k	$Z=a R^b$
Ile-Ife, Nigeria	5.91×10^{-4}	624	4.5585	$461 R^{1.31}$
Nairobi, Kenya	4.727×10^{-4}	400	4.7754	$461 R^{1.31}$
Douala, Cameroon	2.237×10^{-4}	732	5.9737	$461 R^{1.31}$

2.5 Input parameters used for modeling

The modeling of the modified 3-D cell model requires some input parameters, which include the local meteorological information of the location, and the geometrical and electrical properties of the link.

Inputs for the electrical characteristics of the link include; antenna gains, antenna polarization, 3dB- beam-widths, operating frequency and polarization decoupling factor M. The geometrical information with respect to a common volume reference system include; antenna pointing and distance between the stations. The meteorological information required includes $0^{o}C$ isotherm height, cumulative distribution of point rainfall rate P (R) and water vapour density. The additional input information needed are; the relationship between specific attenuation to rain rate, relationship between radar reflectivity to rain rate and the deviation from Rayleigh scatter.

In this study the lognormal distribution for the drop size distribution (dsd) is employed. Rayleigh scattering correction takes care of the shape factor at frequencies higher than 10GHz. The parameters needed to compute the bistatic cross-section (σ_{bi}) for deformed raindrops (for thunderstorm rain type) in tropical locations are obtained from Ajewole, (1997). The attenuation occurring on the bistatic link is approximated to consist essentially of attenuation along the path from the transmitting station to the common volume, and from the common volume to the earth station receiver in the region below h_{FR}, even though this is very small (Ajewole et al., 1999). The main contributors are rain and atmospheric gases (oxygen and water vapour). While the 3-D algorithm used, utilized the ITU-R, recommended procedure for computing attenuation due to atmospheric gases, rain attenuation along the path is computed using the power law relationship of Olsen, (1993). The basic input parameters used in the process of evaluating the cumulative distribution of transmission loss due to interference in this study are as follows;

2.5.1 Link geometry

This study assumed a fixed path length of 50 – 250km from terrestrial station antenna to the common volume distance.

2.5.2 Electrical characteristics of the link

The satellite earth station terminal is defined as the interfered station. Its antenna is assumed to have a Guassian radiation pattern and with a gain set at 59dB, beam width of 0.18^0, efficiency of 55%, and elevation angle of 55^0 which is the look angle of most satellite receiver systems over the Atlantic Ocean region in Nigeria. The interfering terrestrial system for this study has an elevation angle of 1^0, beam width of 1.6^0 and antenna gain varied from 35-55dB. The antennas are assumed located on the ground, with relative height difference of zero. This assumption allows the lower half of the terrestrial station radiation pattern to be cut off, thus making no contribution to interference. The cumulative distribution of transmission loss is evaluated in the forward direction. Frequency range of interest is 4 – 35GHz, and the parameters for evaluating attenuation using the power – law expression, for thunderstorm rain type is assumed. Only the Vertical polarization is investigated in this study because the highest value of coupling occurs whenever both transmit and receive systems are vertically polarized (Awaka et al., 1982).

2.5.3 Meteorological parameters

Convective tropical rains that are usually generated within the cumulonimbus clouds, are convective, and can consist of many active centers with strong up- and down drafts. They are also usually characterized by high rainfall intensity, and are sometimes accompanied by thunderstorm.

In Nigeria, Kenya and Cameroon, the mean freezing height under raining conditions (h_{FR}), is assumed to vary from 4.54 - 4.79Km,because even from eqn. (2.18a), h_{FR} is expected to remain constant throughout the region, so the measured value for Nigeria has been adopted for the locations. The mean annual cumulative distribution of point rain rate P (R) measured at the

locations are used to calculate the cumulative distribution of transmission loss. R^f is 624mm/h for Ile-Ife, 400mm/h for Nairobi and 732mm/h for Douala (four times the maximum rain rate). Average water vapour of $20g/m^3$ is assumed to calculate attenuation due to absorption by atmospheric gases ITU-R, (1997) while a water temperature of 20°C was assumed to calculate the refractive index of water using the method described by Ray, (1972). The measured cumulative distributions of point rain rate at the locations are taken respectively: for Nigeria from the work of McCarthy et al., (1994a), for Cameroon from McCarthy et al., (1994b) and for Kenya from McCarthy et al., (1994c).

CHAPTER THREE

3.0 RESULTS AND DISCUSSION

The modified Capsoni-3-dimentional rain cell model has been used to calculate the statistics of the transmission loss, for terrestrial propagation path length to common volume r_1 (fig2.1) ranging from 50 – 250km. This chapter discusses the results obtained from the computation.

3.1 The Common Volume (CV)

The equivalent satellite - to- common volume distance and terrestrial receiver (r_1 andr_2), and the height of the common volume corresponding to each terrestrial propagation path length are shown in table 2.1 and they are calculated only once for a geometry regardless of the other input parameters, and the horizontal extent of the rain cells. In general, CV increases approximately linearly with increasing antenna separation. When the station separation is longer than 204km (r_1 greater 200km), the common volume is in the ice region, where ice scattering is the dominant scattering mechanism. Indeed, it is only the wanted signal that will be affected by the attenuation in the ice region, while the interfering signal will be less affected. On the other hand, when the CV is below h_{FR}, both the interfering and the wanted signals will be affected to the same extent by the attenuation. Hence, a CV above h_{FR} is subject to a considerably lower transmission loss (higher interference from the interfering signal) compared to one below h_{FR} despite the decrease of Z at a rate of 6.5dB/km above the h_{FR} The same geometries used by Ajewole, (2003) are assumed in this study.

3.2 Comparison of the transmission loss for varying terrestrial antenna station-to-common volume distance.

Figure 3.1 shows an example of the variation of cumulative distribution of the transmission loss with terrestrial station to common volume distance at percentages of occurrence ranging from 0.1 to 0.001, frequency of 16GHz and terrestrial station gain of 45dB. In all the three stations, the results show that the transmission loss increase gradually with distance from the terrestrial antenna to the common volume at all time percentages.

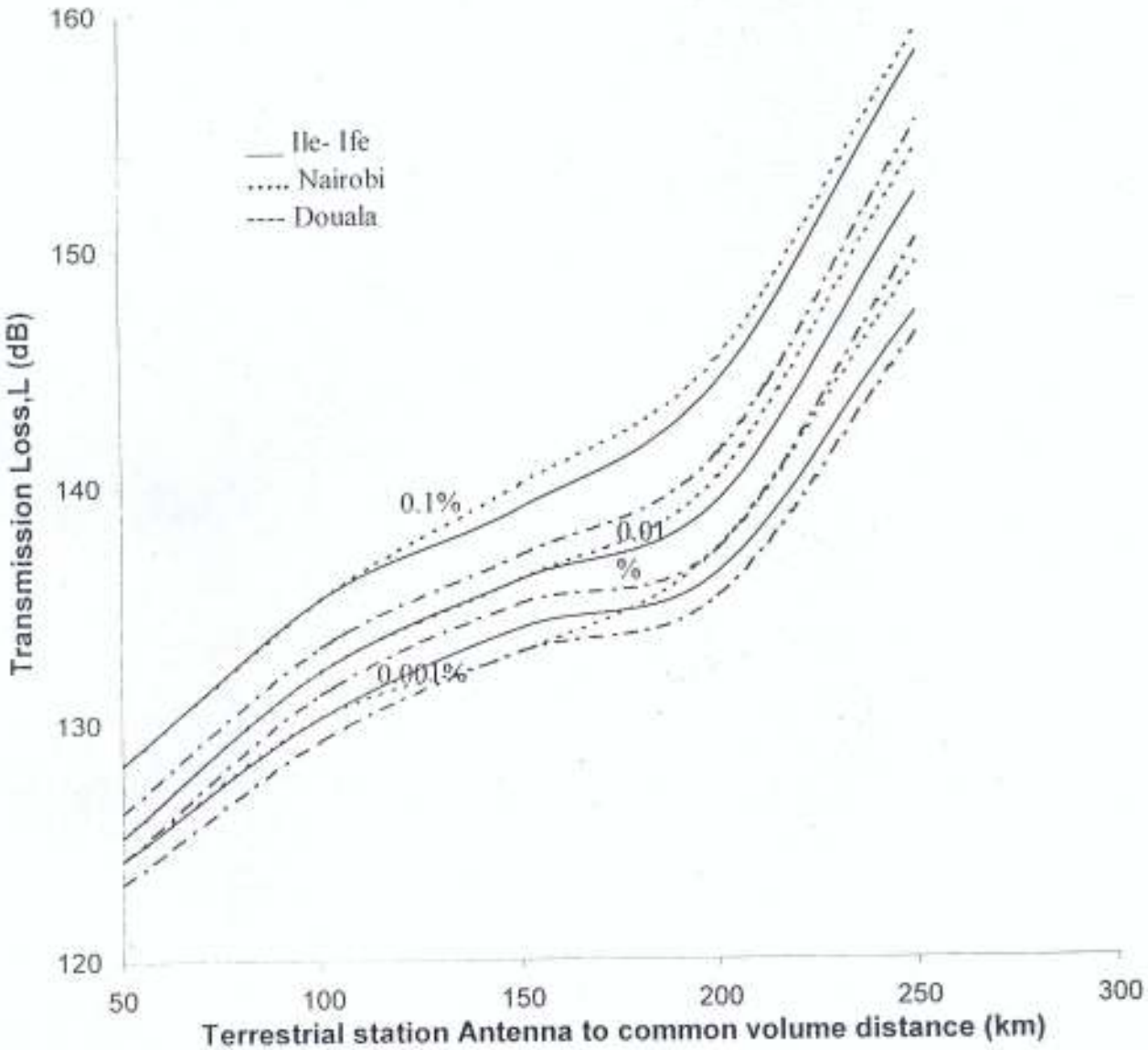

Fig. 3.1 Comparison of the transmission loss with terrestrial antenna station to common volume distance at the locations and varying percentage times

This implies less interference in the satellite receiving system. This trend was observed at other frequencies, but, when the station separation is longer than 204km, the slope of the curve of transmission loss for the various percentages of time becomes steep due to the decrease in radar reflectivity factor in the ice region. This is in good agreement with the result of Ajewole, (2003). The transmission loss for Ile-Ife varies from about 124.3dB to 158.3dB;Nairobi result varies from about 124.3dB to 159.3dB while it is 123.3dB to 155.3dB in Douala. Lower values of transmission loss in Douala, Cameroon signify high interference in the satellite system. This is due to the high rain rates and high average annual rain accumulation of about 4110mm in the region as percentage of time decreases compared to about 930mm and 1400mm in Nairobi and Ile- Ife respectively, (McCarthy et al., 1994a-c and Ajewole, 2003)

The comparison presented in figure 3.2 shows that transmission loss is at the level of 158.4dB at a frequency of 20GHz in Douala, while it is 160.4 and 161.4dB at the same frequency in Ile-Ife and Nairobi respectively. This suggests high interferences in Douala, Cameroon. Transmission loss L, increased gradually with increasing station separation for frequencies up to 16GHz for station separation less than 204km, but at station separation greater than 204km, the slope becomes steeper due to the decrease in radar reflectivity factor in the ice region. At the higher frequency of 20GHz, the transmission loss is significally higher than at the lower frequencies. Though not shown here, the same result is also noticed at frequency of 34.8GHz,this is due to the strong path length attenuation and at 250km to the common volume due to the rapidly decreasing radar reflectivity.

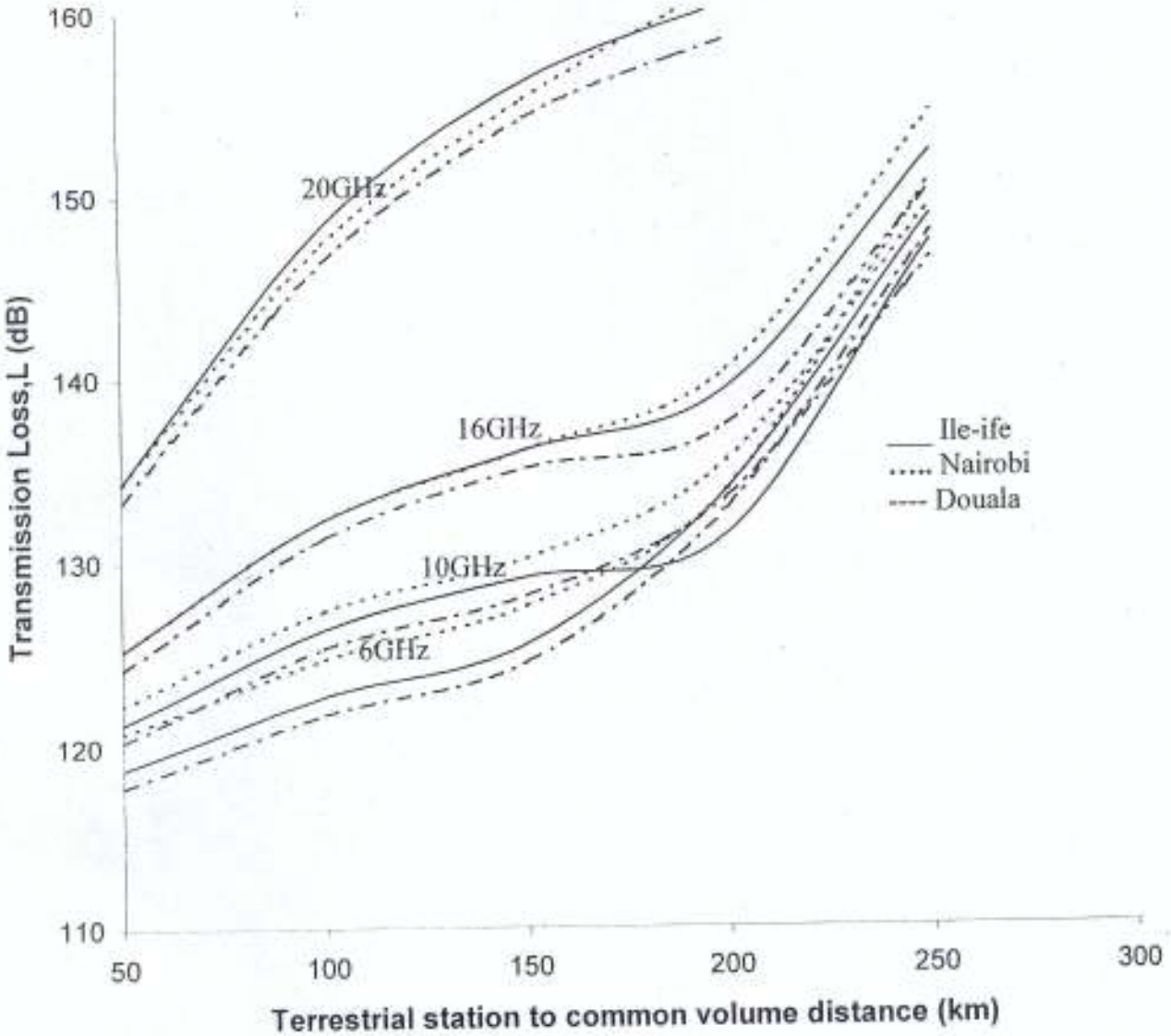

Fig.3.2 Comparison of the transmission loss with terrestrial antenna station to common volume distance at the locations, 0.01% of time and varying the frequencies.

3.3 Comparison of the transmission loss with frequency

The influence of varying the frequency on the computed transmission loss is examined over varying terrestrial propagation path length at time percentages of 10^{-1} to10^{-3}%. The comparison is shown in figures 3.3 and 3.4 over short and long path lengths for frequencies 4, 8, 10, 16, 20, and 34.8GHZ.The transmission loss curves for the short path length (50km) varies from about 117.3dB to 135.3dB, 118.3 to 136.6dB and 119.3 to 137.3dB in Douala, Ile- Ife, and Nairobi respectively while it is about 143.3dB to 164.4dB, 145.4dB to 165dB and 143.3dB to 166.4dB in Ile-Ife, Nairobi and Douala respectively when the path length is 250km.At frequencies of 20 and 34.8GHz, the transmission loss is significantly higher than at other frequencies for these path lengths. Transmission losses at other frequencies are bounded in a narrow range.

3.4 Comparison of the transmission loss with terrestrial antenna gain

The comparison of the transmission loss is made at terrestrial antenna gain varying from 35 – 55dB for signal passage through thunderstorm rain type and at time percentages of 10^{-1}- 10^{-3}%. The comparisons are also made at frequencies of 6GHz and 20GHz for short and long path lengths to the common volume as presented in figs.3.5 – 3.7. In figure 3.8, the transmission loss for other time percentages is omitted due to an assumption by the algorithm used to discard coupling less than –180dB for practical reasons. The results suggest that in general for a given terrestrial gain, the cumulative distribution of transmission loss increase with increasing probability (decreasing channel availability). Also, transmission loss decreases linearly with increasing antenna gain for a given outage margin (percentages of time). For example, at frequency 6GHz, while the transmission loss decreases to a level of about 105.8, 106.8 and 107.8dB in Douala, Ile- Ife and Nairobi respectively, at very high probability (10^{-3}) and at short path length (50km); the minimum transmission loss is at the level of 122.3dB at a frequency of 20GHz at the same path length.

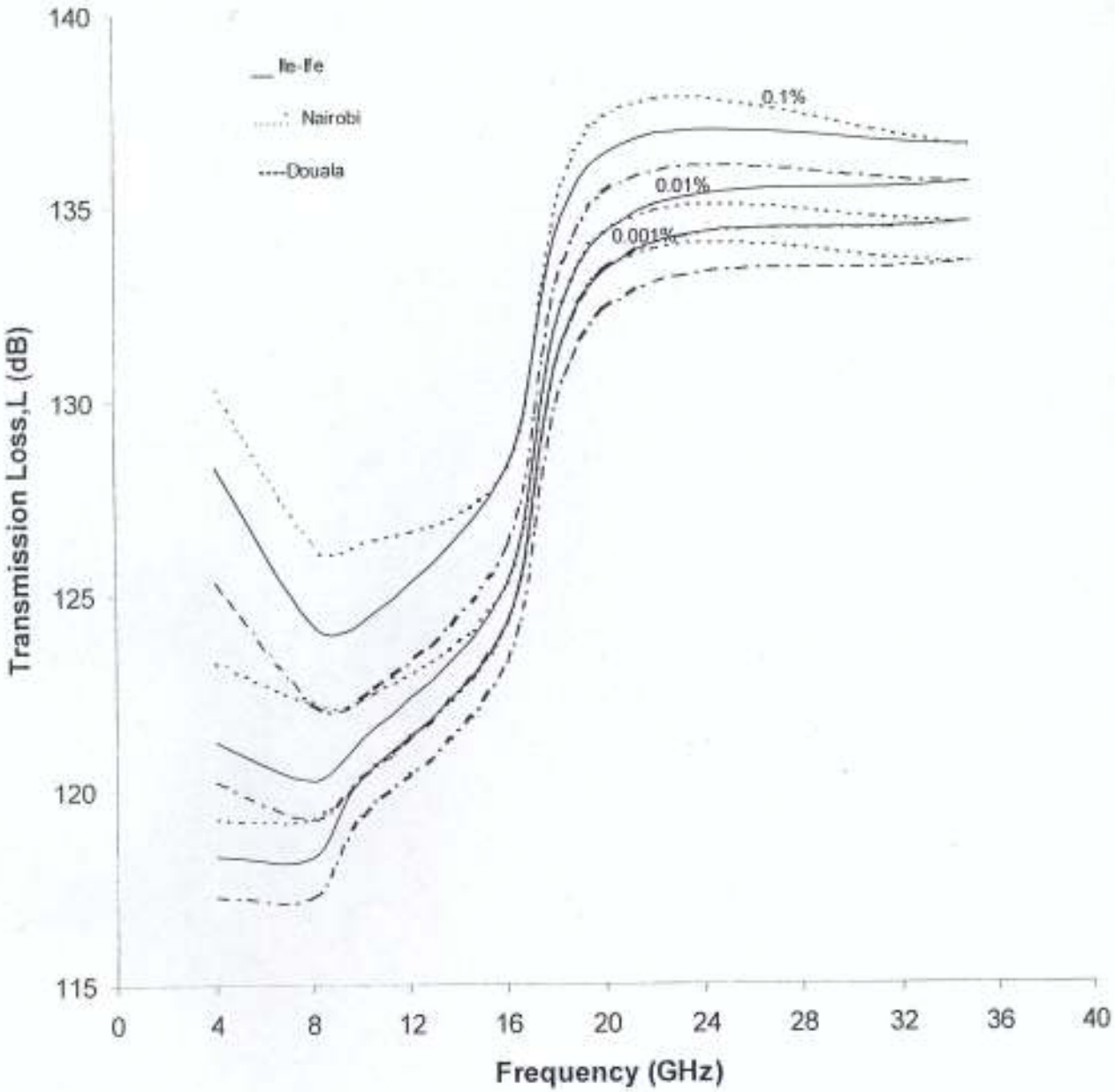

Fig.3.3 Comparison of the transmission loss with frequency computed at the locations, terrestrial antenna station to common volume distance of 50km (short path length) and varying percentage times.

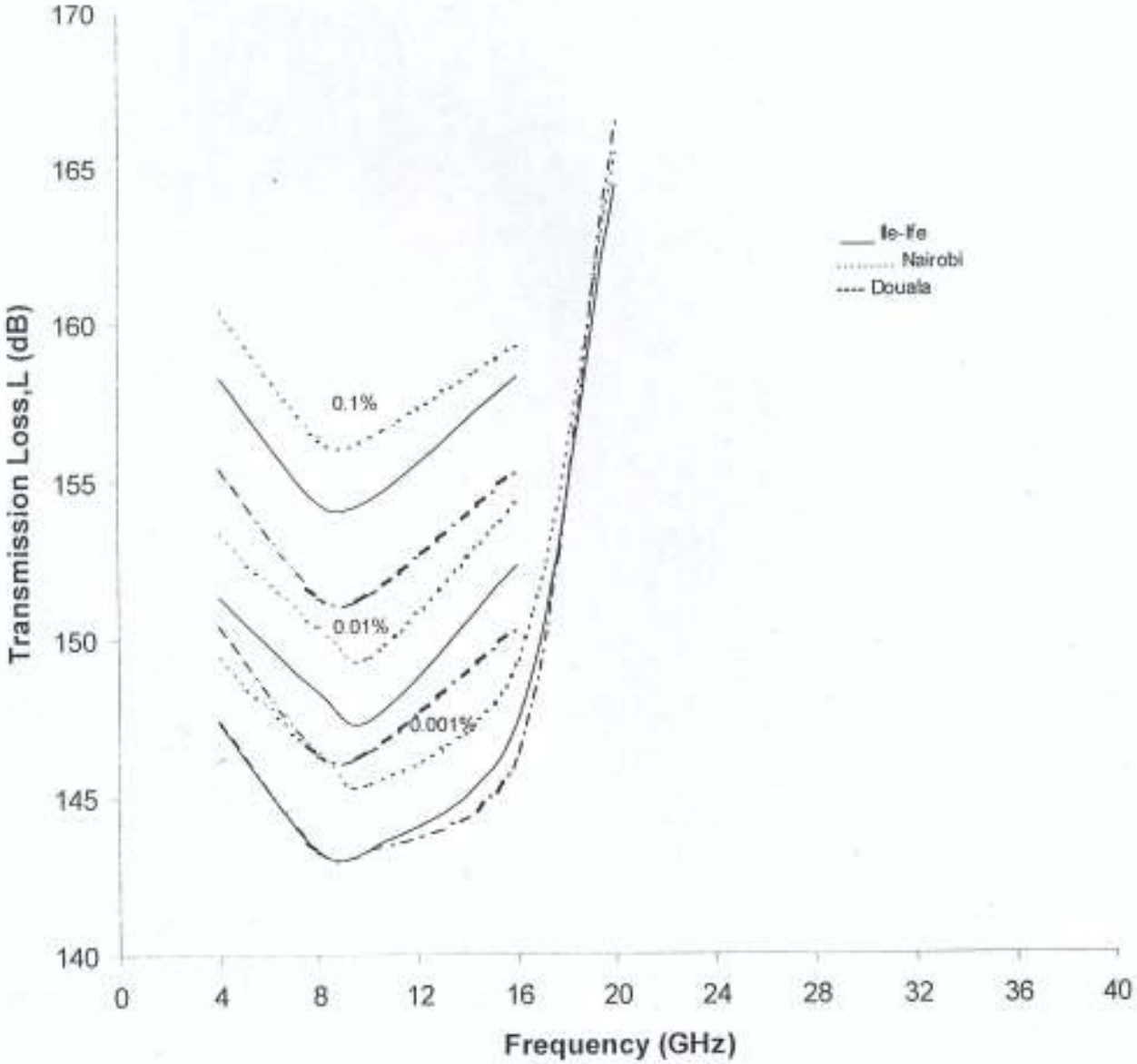

Fig.3.4 Comparison of the transmission loss with frequency at the locations, terrestrial antenna station to common volume distance of 250km (long path length) and varying percentage times.

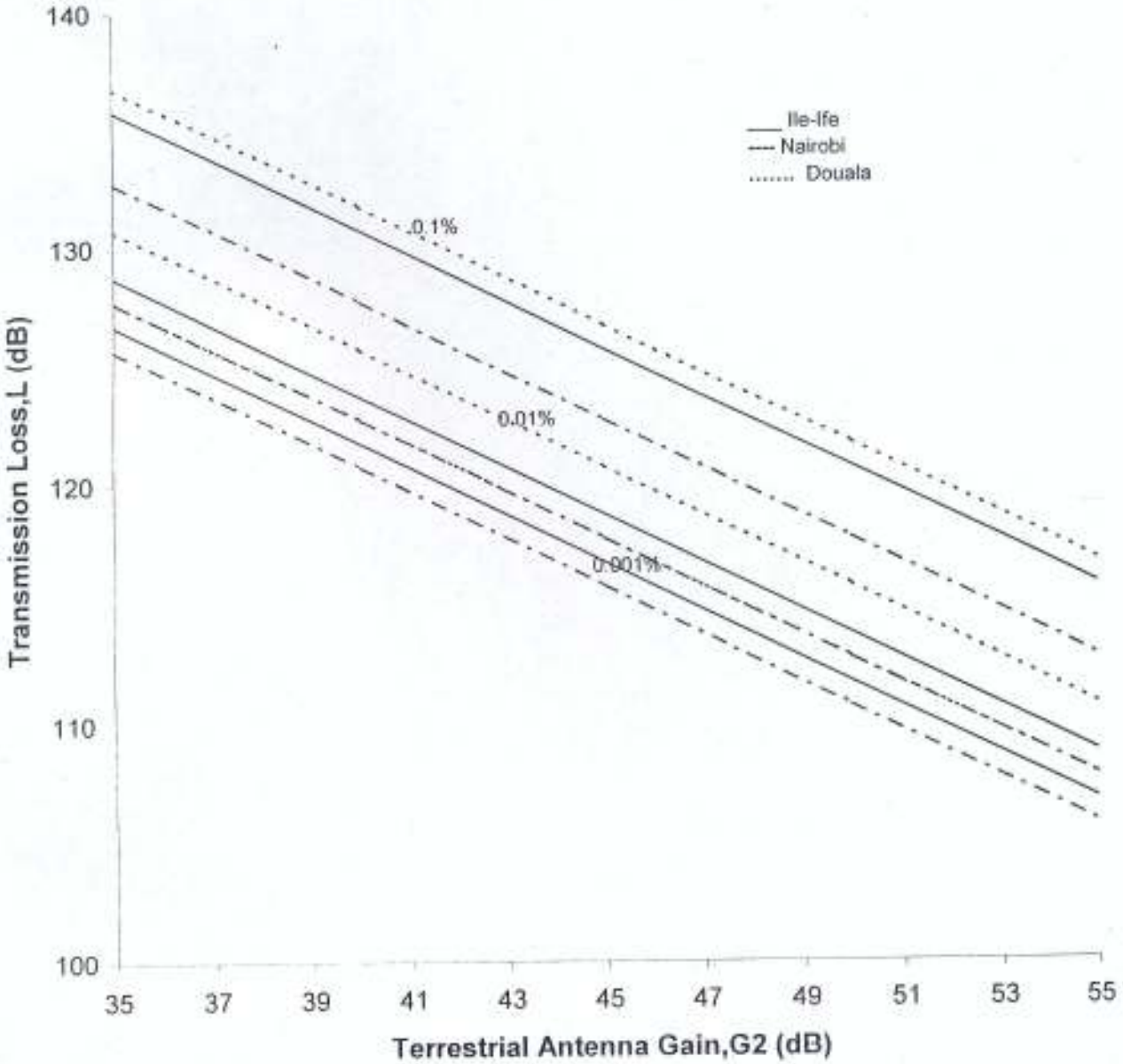

Fig.3.5 Comparison of the transmission loss with terrestrial antenna gain at the locations, frequency of 6GHz,terrestrial antenna station to common volume distance of 50km (short path length) and varying percentage times.

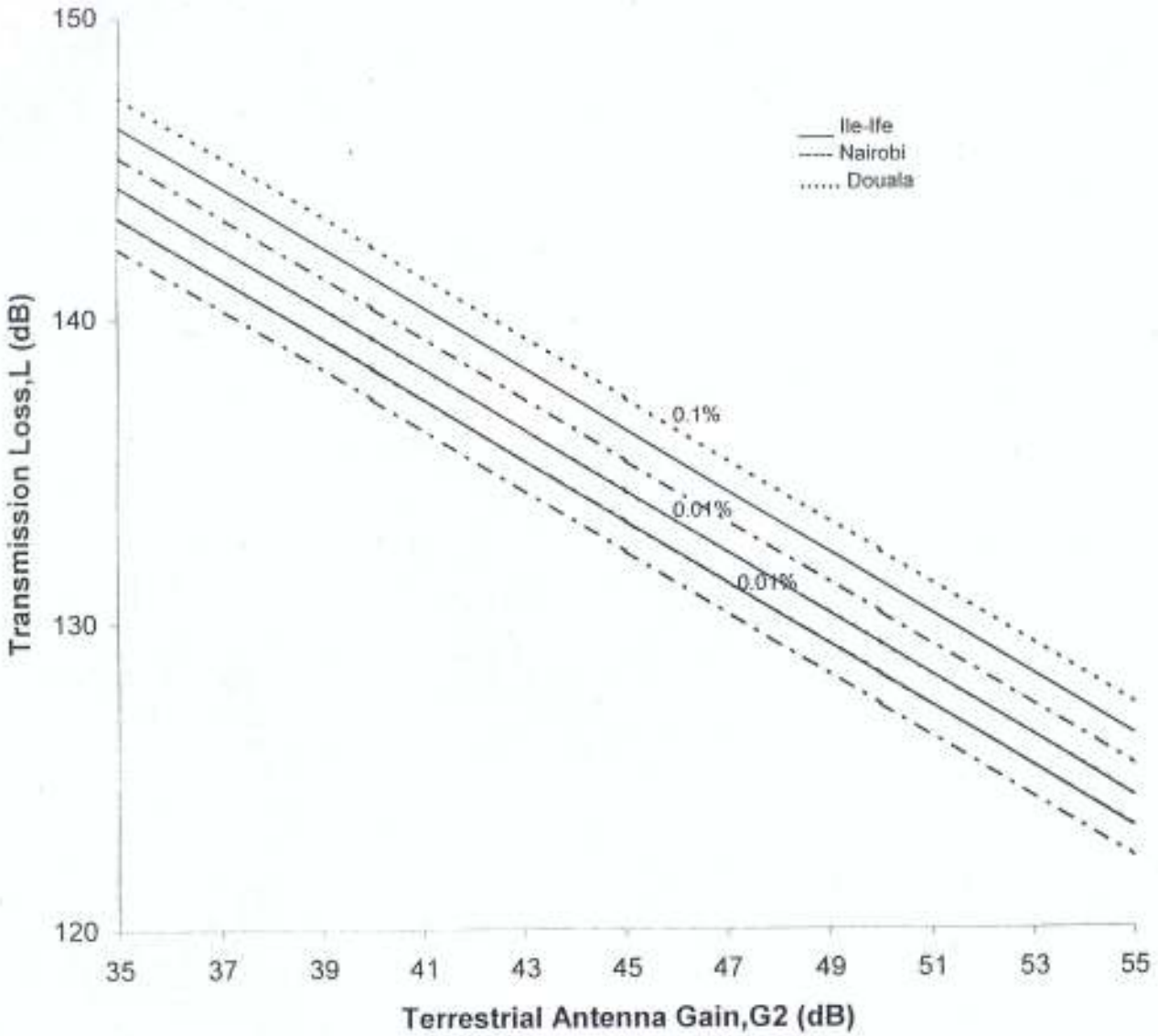

Fig.3.6 Comparison of the transmission loss with terrestrial antenna gain at the locations, frequency of 20GHz, terrestrial antenna station to common volume distance of 50km (short path length) and varying percentage times.

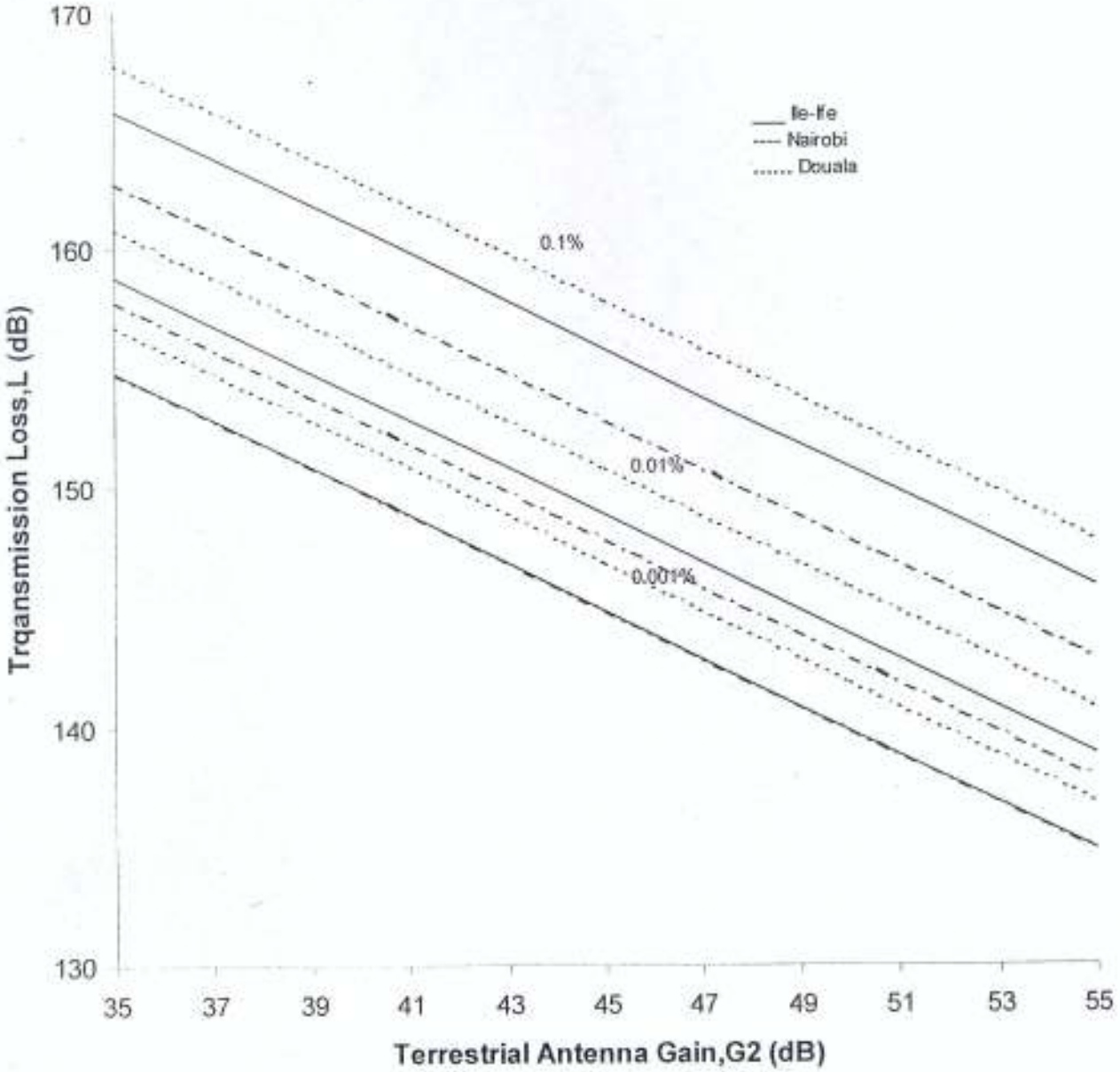

Fig.3.7 Comparison of the transmission loss with terrestrial antenna gain at the locations, frequency of 6GHz, terrestrial antenna station to common volume distance of 250km (long path length) and varying percentage times.

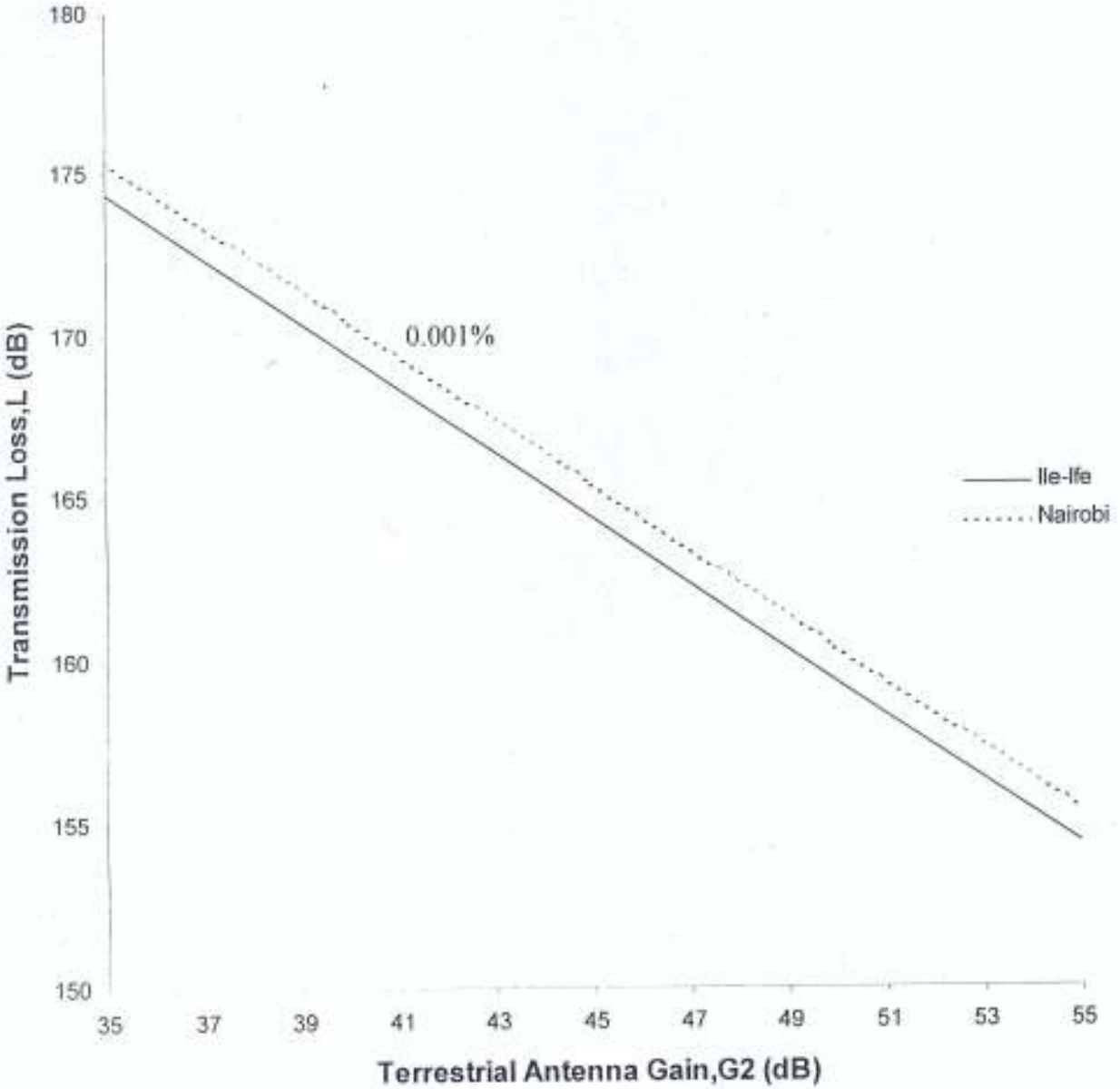

Fig.3.8 Comparison of the transmission loss with terrestrial antenna gain at the locations, frequency of 20GHz, terrestrial antenna station to common volume distance of 250km (long path length) and varying percentage times.

At long antenna separation (250km) and frequency of 6GHz; the minimum transmission loss is at the same level of 134.8dB at both Douala and Ile Ife while it is about 136.8dB at Nairobi at very high probability of 10^{-3} %. Also, the minimum transmission loss is at 154.4dB at a frequency of 20GHz at the same station separation. Interference received from the terrestrial station by the earth station receiver will be lower in Douala and Ile- Ife compared to Nairobi. There is possibility of severe interference in the satellite receiver at the short separation between the antenna systems, more so that the total attenuation is small at low frequencies. Also at long path length of 250Km, common volume is above the freezing height level, indicating that attenuation due to the ice region also contributed to the interference.

3.5 Comparison of the transmission loss with percentages of time

The results of the transmission loss were also compared with % of occurrence ranging from 10^{-1} to 10^{-4}. The comparisons were made at frequencies of 6,10,16 and 34.8GHz and terrestrial gain of 45dB. Typical result short path length of 50km is shown in figure 3.9. The transmission loss curves for the short path length varies from about 114.8 to 136.6dB, 115.8 to 136.6dB and 114.8 to 135.6dB for Ile –Ife, Nairobi, and Douala respectively. Though not shown here, the transmission loss varies from about 141.4 to 160.6dB, 143.4 to 160.6dB and 141.4 to 160.6dB for Ile –Ife, Nairobi And Douala respectively when the path length is 250km. Over these path lengths, and at a frequency of 34.8GHz, the transmission loss is significantly higher than at other frequencies due to the strong path length attenuation and in addition at 250km due to the rapidly decreasing radar reflectivity in the ice region. Transmission losses at other frequencies are bounded in a narrow range.

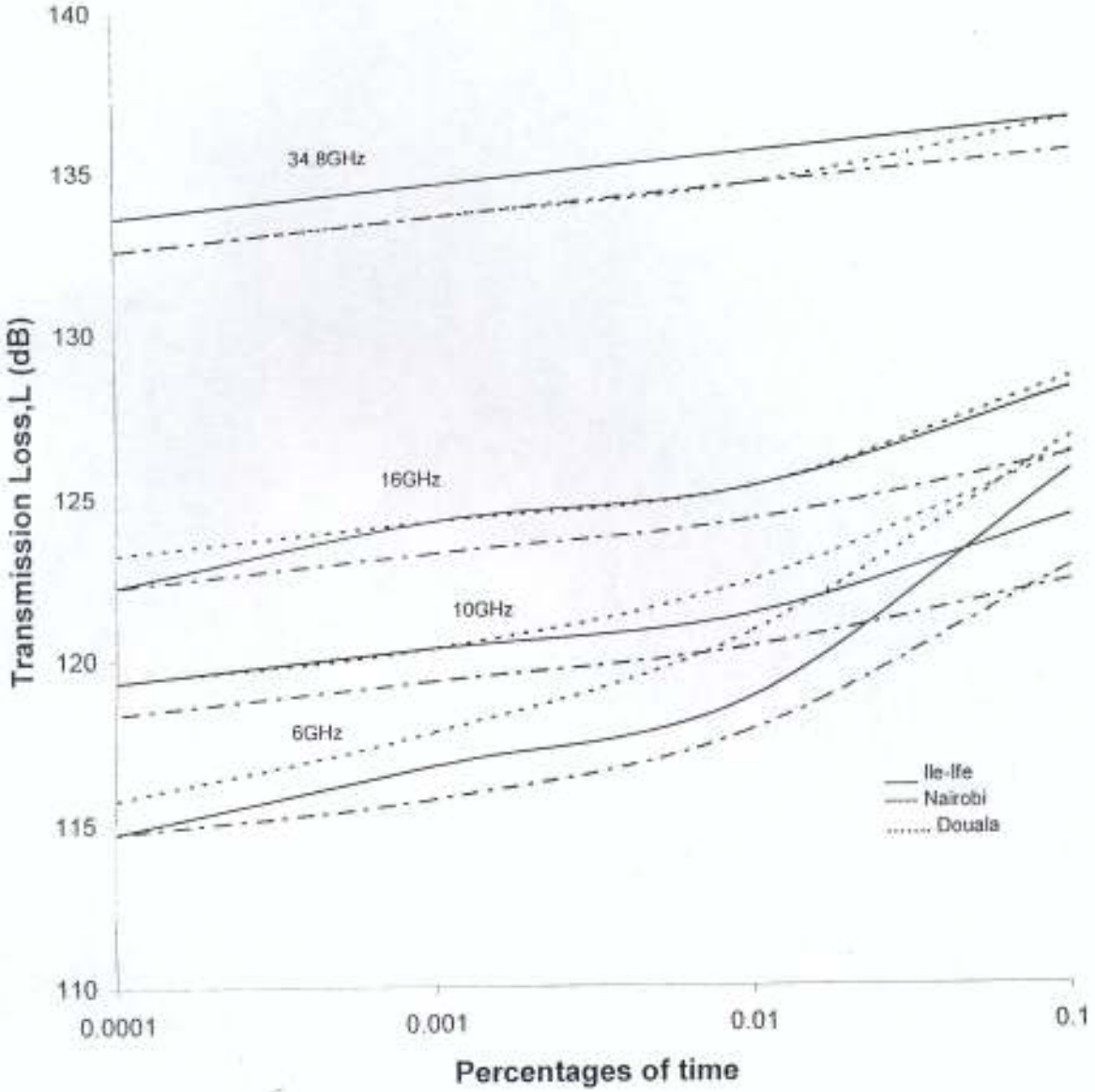

Fig. 3.9 Comparison of the transmission loss with % of time at the locations, terrestrial antenna to common volume distance of 50km (short path length) and varying the frequencies.

3.6 Comparison of percentage difference of transmission loss between Kenya, Cameroon and Nigeria.

Ajewole et al,. (1999), computed transmission loss for Nigeria. They assumed two-elevation angles of 55^0 and 23^0 and two-rain types, thunderstorm and shower. In the study, the mean annual rain rate distributions were used for shower, while the mean worst month distributions were used for thunderstorm rain. Furthermore, Ajewole, (2003) computed transmission loss for elevation angle of 55^0, terrestrial gain of 40.5dB and three rain types (Widespread, Shower and Thunderstorm). This latter study was based on two rain cell models, the Capsoni 3-D cell model and the Awaka (1989) model. Since much work has been carried out on Nigeria, percentage difference can be made between the Nigerian results and the other sub-Saharan tropical locations (Kenya and Cameroon) considered in this study.

The percentage differences are reported only for 0.01 percentage of time, since this is the time percentage unavailability used for most designs in satellite telecommunications.

Fig 3.10 shows the results comparing the percentage difference between Nigeria and other locations. curves below the Nigerian data indicate that the results for Nigeria are lower by percentages indicated on the curve while curves above indicate that the results for Nigeria are higher by the percentages shown.

The results as presented in figure 3.10 shows that while varying the transmission loss with terrestrial antenna to common volume distance, the transmission loss is higher in Douala by less than 2%, and lower in Nairobi by less than –1.5%. These results show that a good agreement exists between the Nigerian data and these other stations. Though not shown here, the results of varying the frequencies, and gain characteristics of the transmission loss show that the percentage difference between the cumulative distribution loss in Nigeria and in Kenya and Cameroon will be less than $\pm 2\%$, whether the path length is short or long.

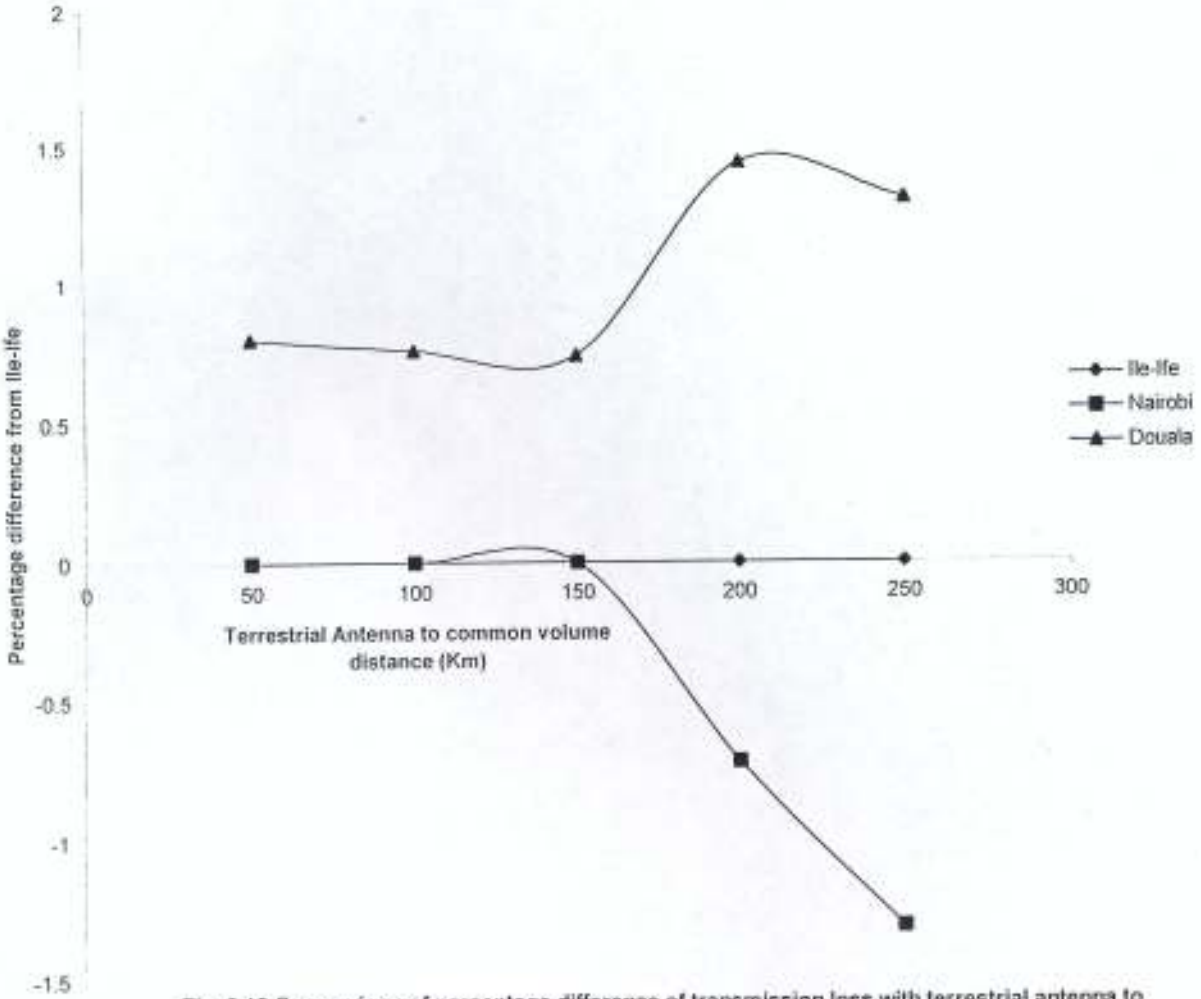

Fig. 3.10 Comparison of percentage difference of transmission loss with terrestrial antenna to common volume distance between Nairobi ,Douala and Ile-Ife for 0.01 % of time

3.7 Evaluation of effective transmission loss, Le.

In this section, the results of some possible effects of the extra attenuation on the wanted satellite signal are presented. In considering interference by rain scatter, statistics of the cumulative distribution of transmission loss alone will not be sufficient to assess the severity of interference at the interfered station. At higher frequencies, that is, above about 10GHz, the wanted signal also suffers from attenuation due to hydrometeor scatter, in addition to signal degradation due to depolarization effects. In locations with intense rain activity, the attenuation along the wanted path could be larger than the maximum link margin so that the satellite link would be out of service whatever the level of interference (Capsoni and D'Amico, 1997). However, when the link margin is not exceeded, the extra attenuation by rain has the potential of increasing interference in the wanted signal by reducing signal- to- noise ratio in the receiver terminal. The effect of the extra attenuation is described by the effective transmission loss, Le, defined as the difference between the transmission loss and the extra attenuation, on the basis of joint dependence on the statistics of the transmission loss and the attenuation. The effects of varying effective transmission loss with some other parameters are discussed in what follows.

3.7.1 Comparison of the effective transmission loss (Le) for varying terrestrial system-to-common volume distance.

The results of the variation of the effective transmission loss terrestrial antenna distance to the common volume and percentages of time ranging from 10^{-1} to 10^{-3}, frequency of 16GHz and terrestrial station gain of 45dB are presented in fig. 3.11. The effect of the extra attenuation due to rain along r_2 is quite significant. At a station separation of 50.7km (terrestrial station-to-common volume distance of 50km) and % of time of 10^{-3}, the effective transmission loss is about 99.3dB, 106.3dB and 85.3dB for Ile-Ife, Nairobi and Douala respectively. Le is highest at Nairobi, and lowest at Douala. Lower values in Douala signify high interference in the satellite system. This is due to the high average annual rain accumulation of about 4110mm in Douala compared to about

930mm and 1400mm in Nairobi and Ile-Ife respectively. Generally speaking, Le increased with increasing antenna separation.

Next, we consider the variation of effective transmission loss with terrestrial to common volume distances at some frequencies, for 0.01% of time. The result is as presented in figure 3.12.For a station separation of 50.7km; Le is about 107.6dB at a frequency of 34.8GHz for Ile-Ife, Nigeria while it is 114.6 and 92.6dB for Nairobi and Douala respectively at the same frequency and time percentage. The difference between the transmission loss is large when compared at lower frequencies and short station separations. Further at same station separation of 50.7km and frequency of 6GHz, Le is about 117.8dB at Ile-Ife while it is 119.8 and115.8dB for Nairobi and Douala respectively at this same frequency and time percentage of 0.01%. The Ile-Ife result is in agreement with the earlier results of Ajewole, (2003). Regardless of the frequency, Le is lower in this study in Douala when compared with the other locations. This means that there is a stronger interference effect due to larger increase of attenuation along the wanted path in Douala. Also, the cumulative distribution of Le shows a significant dependence on the local metrological point rain rate distribution. Hence, the effect of the larger accumulated water in Cameroon is a strong factor responsible for the larger extra attenuation.

Figs.3.13 and 3.14 show the comparison of the results of Le at some frequencies and percentage time unavailability for both short and long path lengths. For the probability levels considered (10^{-3} to10^{-1}), Le decreases generally but with a crest around 20GHz frequency. It decreases further after 20GHz.The effective transmission loss increases with increasing percentages of time for short path length (50km). However, at long path length (250km), Le decreases up to 10GHz, but started increasing at the frequency of 16GHz, this is due to the decrease in radar reflectivity factor in the ice region and the strong path length attenuation. However, minimum effective transmission loss still occurs in Douala when compared with other locations.

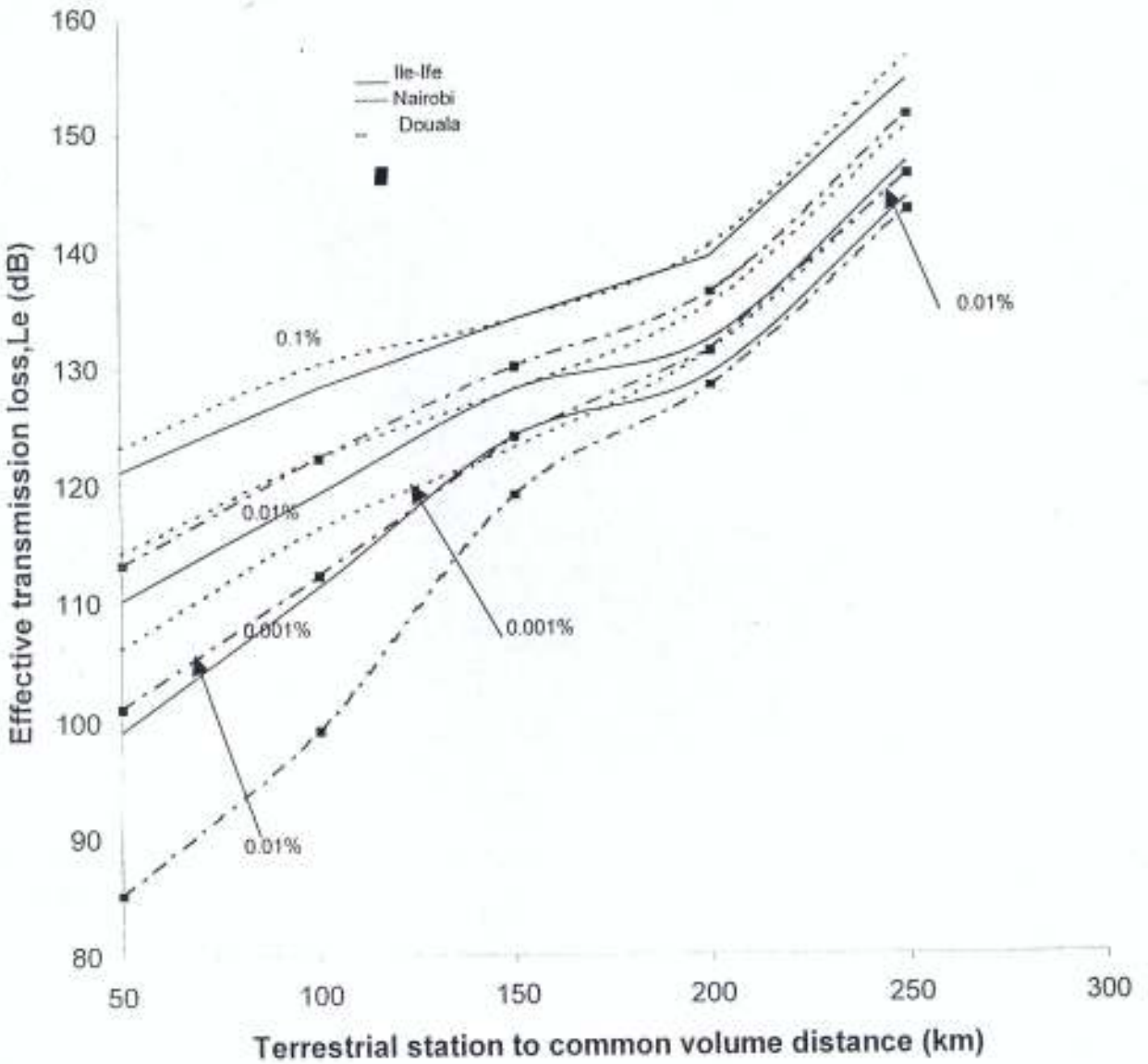

Fig.3.11 Comparison of the effective transmission loss with terrestrial antenna station to common volume distance at the locations, frequency of 16GHz and varying percentage times.

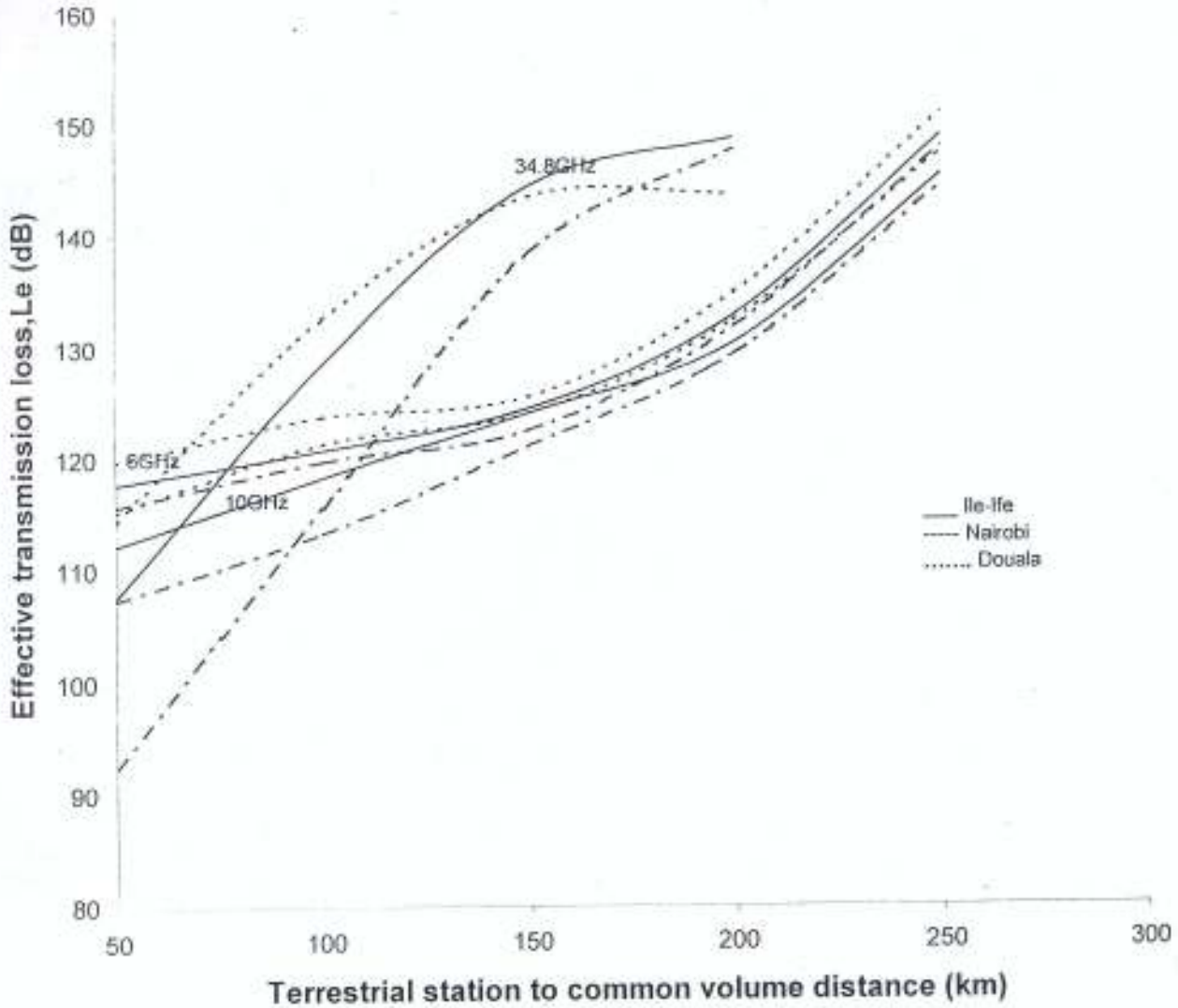

Fig. 3.12 Comparison of the effective transmission loss with terrestrial antenna station to common volume distance at the locations, 0.01% of time and varying the frequencies.

3.7.2 Comparison of the effective transmission loss with terrestrial antenna gain

Figs 3.15 to 3.18 presents the results of the influence of terrestrial antenna gain on the effective transmission loss at some frequencies over short and long terrestrial propagation paths. Time percentages of occurrence ranging from 10^{-1} to 10^{-3} and terrestrial antenna gain ranging from 35 – 55dB are considered. In general, for a given terrestrial antenna gain, the effective transmission loss increases with increasing probability. Also, Le decreases linearly with increasing antenna gain for a given outage margin. For short path length, while Le decreases to a level of 101.8, 103.8, and 105.8dB in Douala, Ile- Ife, and Nairobi respectively at frequency of 6GHz for high availability requirement of 10^{-3}%, Le is at the level of 78.3, 94.3, and 101.3dB for frequency of 20GHz for the same station separation. The difference between Le in the locations is about 2dB at lower frequencies (fig 3.15) while the difference increases to about 16dB at the higher frequency of 20GHz (fig 3.16) for the same % of time. This is due to the fact that the total attenuation is small at low frequencies. However, Le for 10^{-3}% of time occurrence in Nairobi is the same as for 10^{-2} in Douala. When the station separation is 250km at time % of 10^{-3} Le decreases up to the level of 133.8dB (Ile-Ife and Douala) and 136.8dB in Nairobi at a frequency of 6GHz while minimum Le occurs at the level of 154.4 and 155.4dB in Douala and Ile- Ife for frequency of 20GHz.The difference is about 3dB at lower frequency while it is about 1dB at higher frequency.

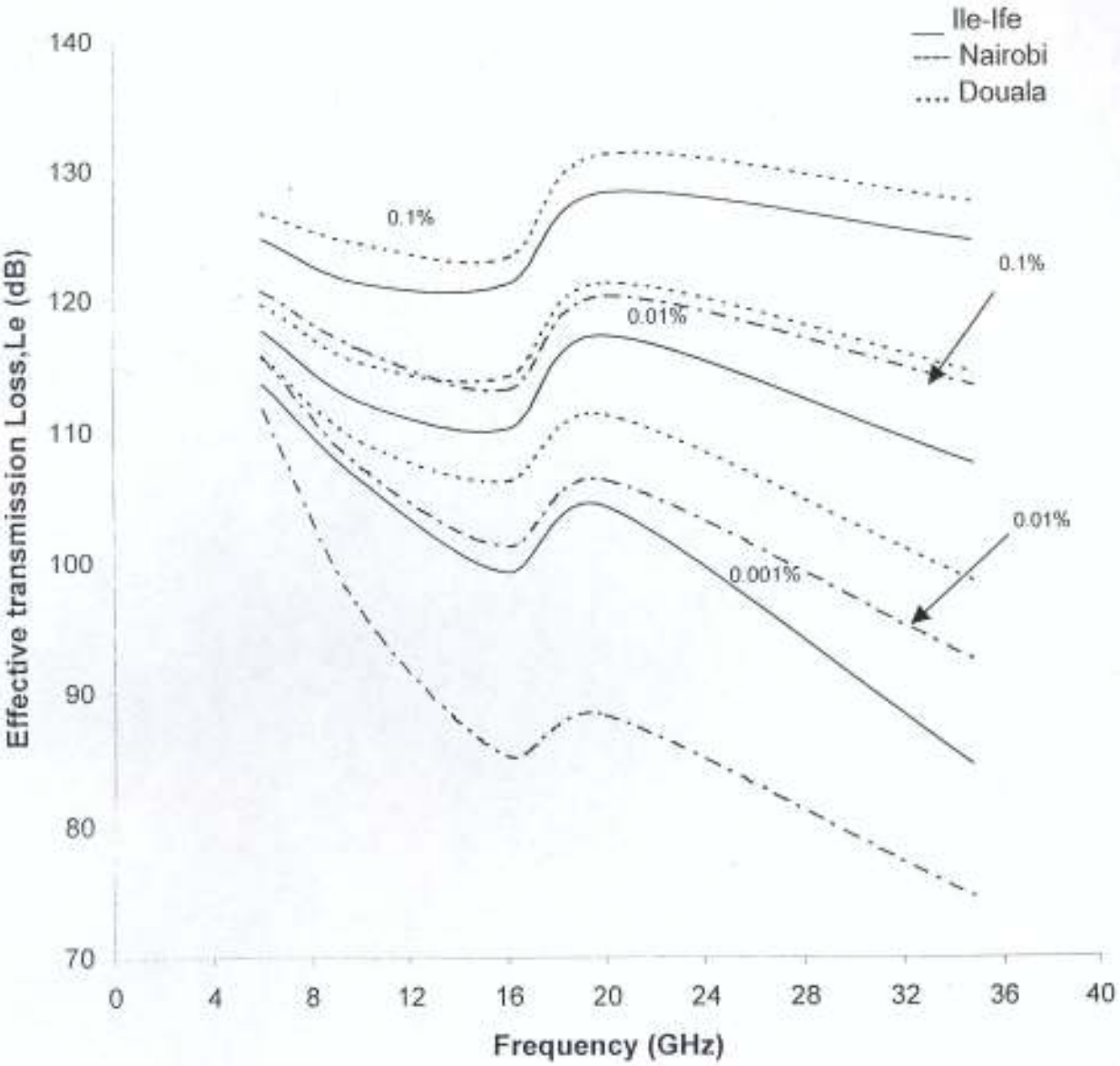

Fig. 3.13 Comparison of the effective transmission loss with frequency at the locations, terrestrial station to common volume distance of 50km (short path length) and varying percentage times.

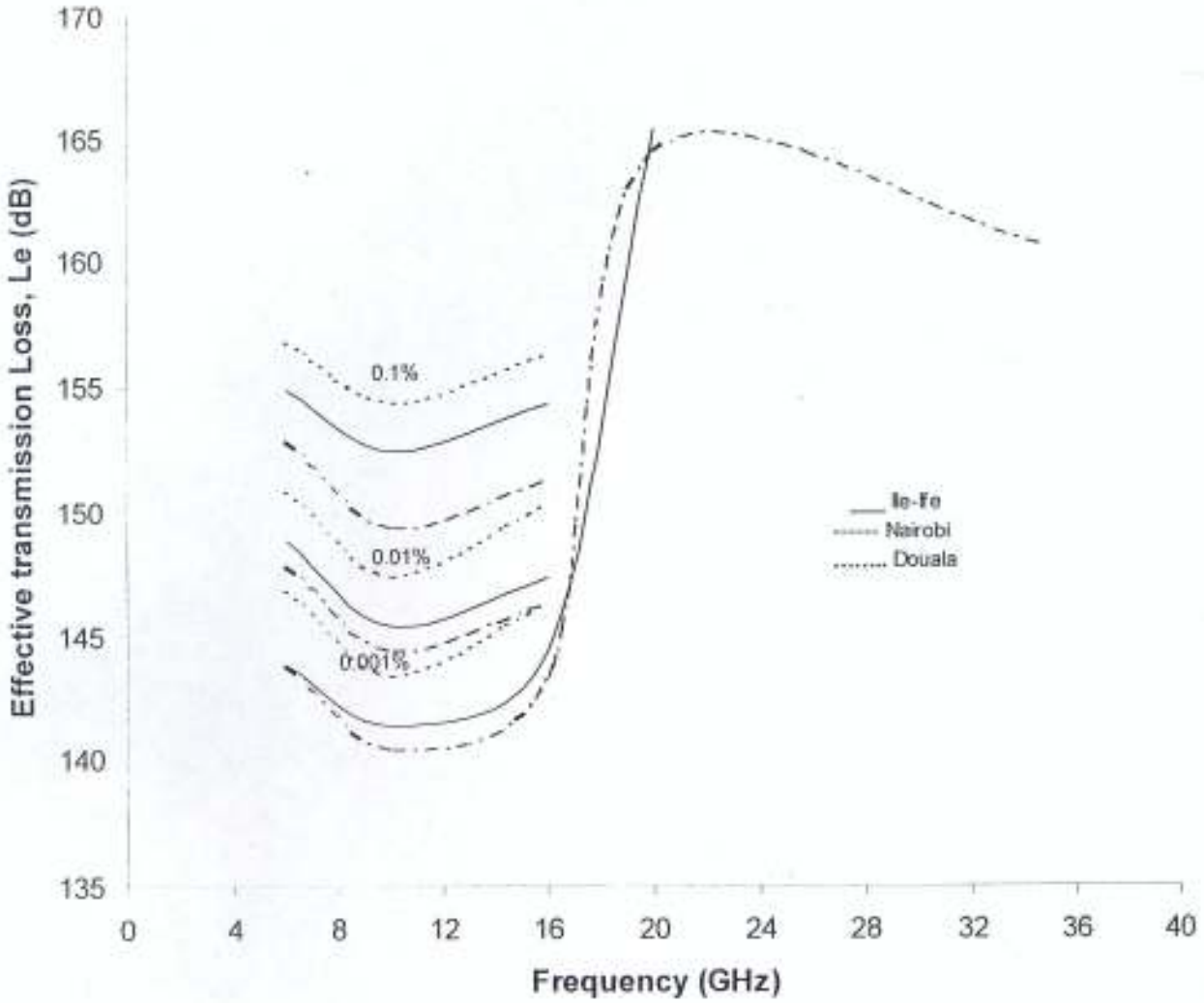

Fig. 3.14 Comparison of the effective transmission loss with frequency at the locations, terrestrial station to common volume distance of 250km (long path length) and varying percentage times.

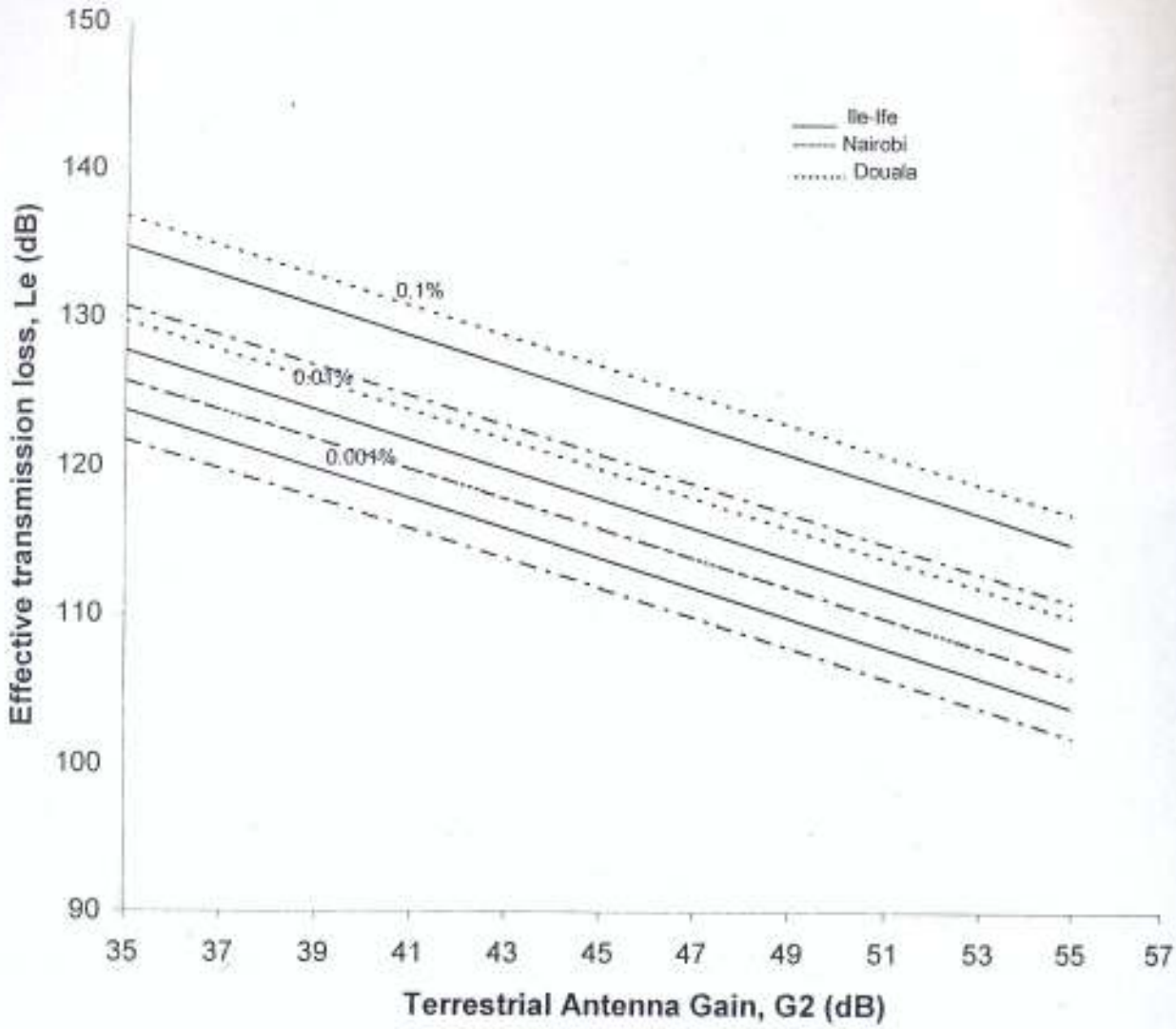

Fig.3.15 Comparison of the effective transmission loss with terrestrial antenna station gain at the locations, frequency of 6GHz, terrestrial antenna station to common volume distance of 50km (short path length) and varying percentage times.

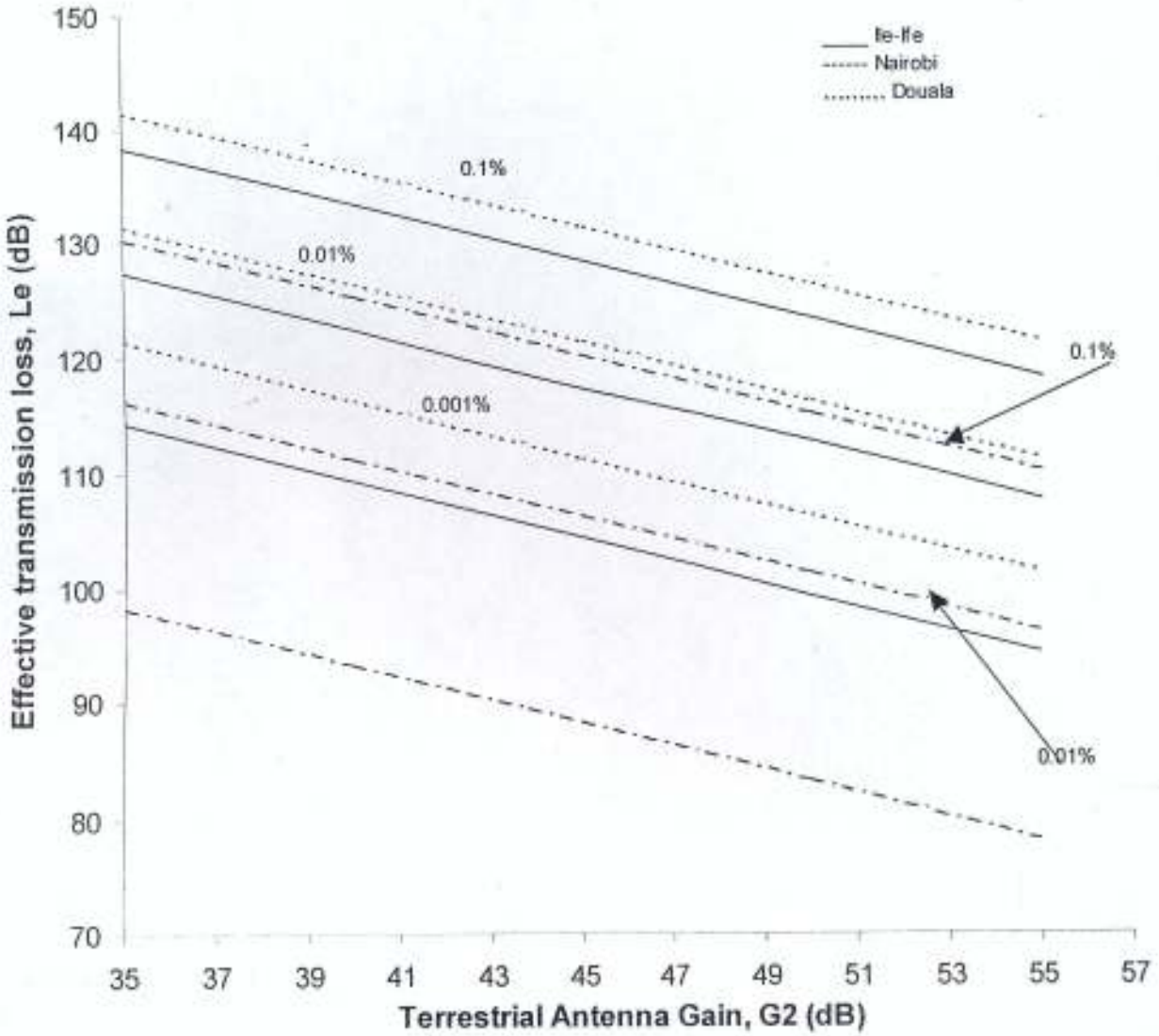

Fig.3.16 Comparison of the effective transmission loss with terrestrial antenna station gain at the locations, frequency of 20GHz, terrestrial antenna station to common volume distance of 50km (short path length) and varying percentage times.

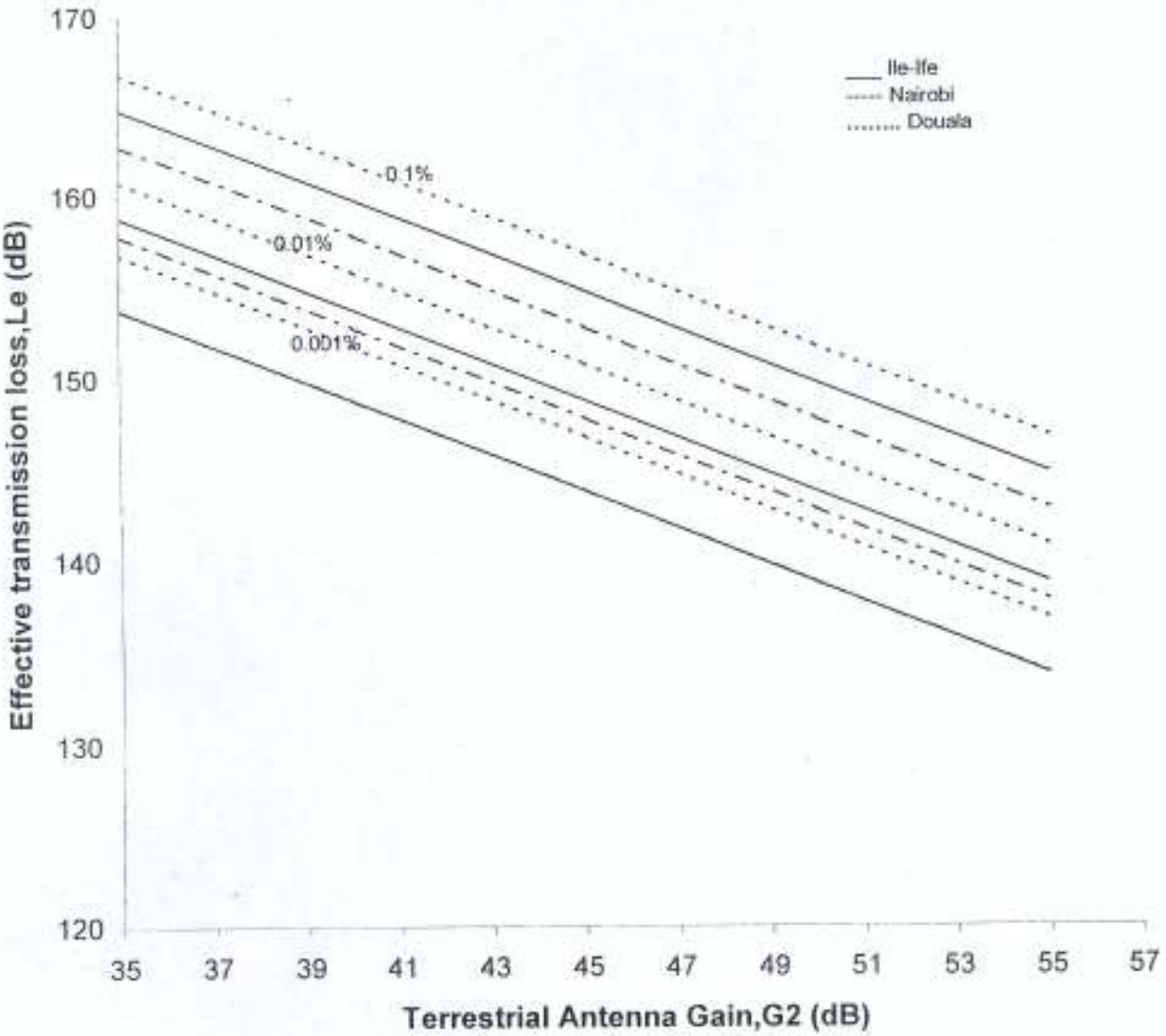

Fig.3.17 Comparison of the effective transmission loss with terrestrial antenna station gain at the locations, frequency of 6GHz, terrestrial antenna station to common volume distance of 250km (long path length) and varying percentage times.

3.7.3 Comparison of the effective transmission loss with percentages of time.

The result as presented in fig 3.19 shows the comparison of the effective transmission loss with time percentages over long terrestrial propagation paths, and frequencies 4, 8, and 16GHz. The effect of the extra attenuation due to rain along r_2 is quite significant. When the path length is 250km Le is about 144.3, 146.3, and 143.3db in Nigeria, Kenya and Cameroon at the same frequency. This result is also in good agreement with Ajewole, (2003).

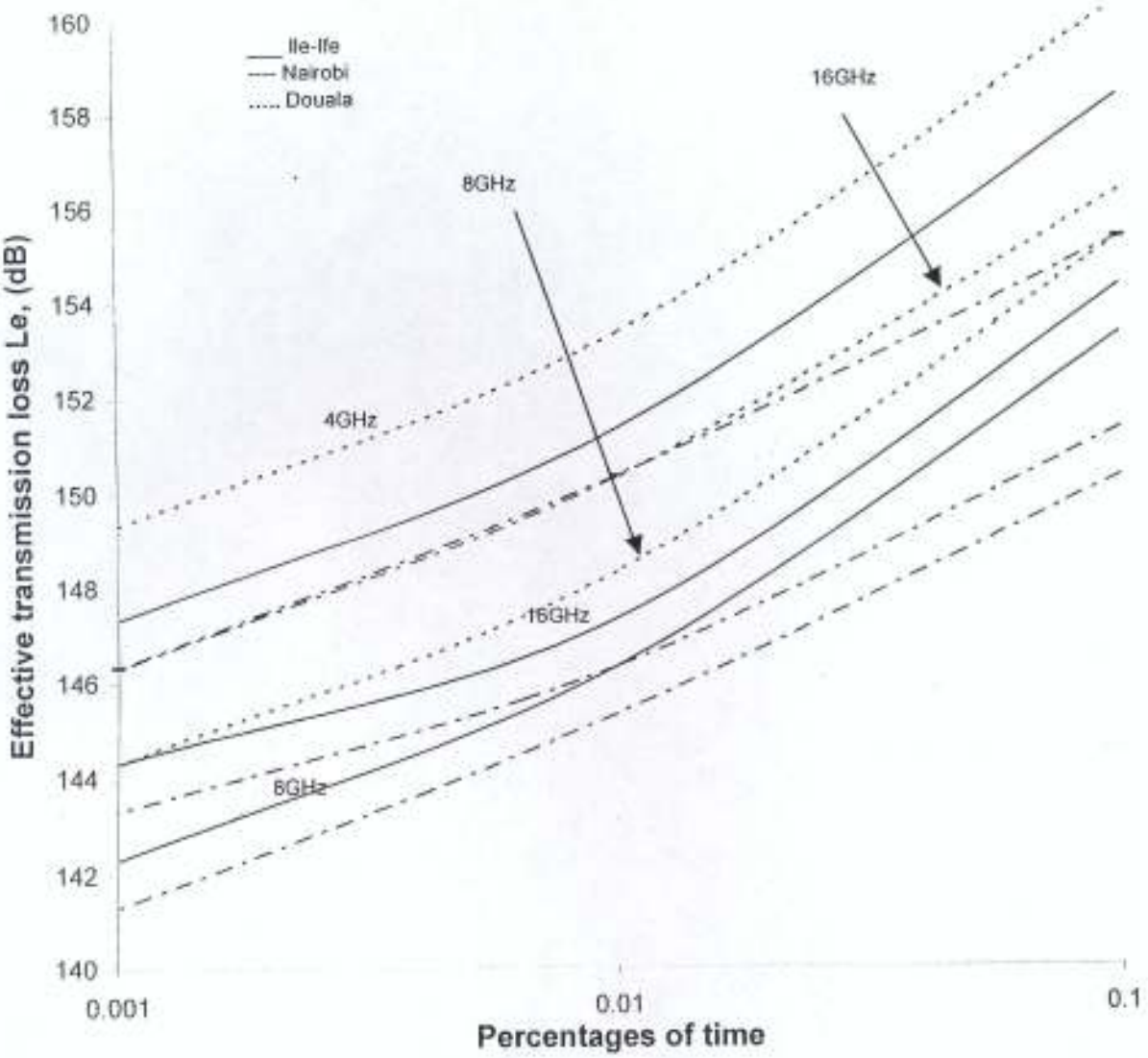

Fig.3.18 Comparison of the effective transmission loss with % of time for at the locations, terrestrial antenna station to common volume distance of 250km (long path length) and varying the frequencies.

CHAPTER FOUR

4.1 CONCLUSION

In this work, the cumulative distribution of the transmission loss L, and the effective transmission loss Le, are calculated using the modified Capsoni 3-D rain cell model. Various other parameters such as frequency dependence, terrestrial station antenna gain, antenna separation etc and their effects on transmission loss have been investigated. The results obtained are compared in the three locations Ile-Ife, Nairobi, and Douala.

The results of the transmission loss with varying station separations obtained in this study for Nigeria are in good agreement with similar ones made by Ajewole et al., (1999) and Ajewole (2003). When compared with the existing results, it was observed that the percentage difference in the transmission loss for station separation is lower in Nairobi by 1.3% compared to Ile-Ife, while it is higher in Douala than Ile-Ife by 1.4% for 0.01% time unavailability. The frequency characteristics of the transmission loss for a given TS gain also show that the percentage difference between Nairobi and Douala is about 2% at occurrence time percentage of 0.01. Further, with these low percentage differences in transmission loss between the stations, the results for Nigeria can be applied with little correction at the other locations. It should be noted however that some common assumptions were made for the stations in the evaluation process, such as similar h_{FR} height, rainfall and meteorological parameters etc. This is due largely to the unavailability of these measured data in Nairobi and Douala.

Since the percentage difference is higher in Douala regardless of the path length, frequency and gain margin, this implies higher interference levels received in Douala. This is due to the higher rain rates and higher annual rainfall accumulation in Cameroon as percentage of time decreases. The evaluation of the effective transmission loss shows that additional rain attenuation will

severely weaken the received signal, which may lead to circuit outage during occurrence of heavy and intense tropical precipitation.

The summary of the computation of the effective transmission loss, Le shows that the values are consistently higher in Nairobi than Douala and Ile-Ife regardless of the parameters being considered.

The results of the present work are in good agreement with those of the previous researchers particularly for Nigeria Ajewole et al., (1999) and Ajewole, (2003). Though the results require experimental validation, it will serve as a database in the planning of an acceptable satellite communication networks particularly in Kenya and Cameroon where there is a dearth of information and data on intersystem interference presently.

4.2 RECOMMENDATIONS

It is recommended that investigation of some radio meteorological parameters such as h_{FR}, raindrop size distribution model, radar reflectivity to rain rate relation, attenuation to rain rate relation, etc in Cameroon and Kenya be carried out as a matter of urgency. Using relevant appropriate parameters for each location to evaluate transmission loss L, and the effective transmission loss Le, may improve the results for the locations. However, it may not be easy to carryout such studies, as it requires up-to-date instrumentation and good substantial funding. Therefore, funding for research from governments and industries is therefore necessary to enhance better telecommunication services in these areas.

Further, a regional or an intergovernmental platform can be created to bring together experts in the field of communication for the purpose of development, quick integration and expansion of telecommunication services across the region.

Since this study focused on vertical polarization, the horizontal polarization can also be investigated.

REFERENCES

Ajayi, G.O and Owolabi, I.E (1987): Rainfall parameters from distrometer drop size measurements at a tropical station, Ann. Telecomm, Vol. 42 No 1-2, p 4-12.

Ajayi, G.O and Barbaliscia, F. (1990): Prediction of attenuation due to rain characteristics of the 0°C isotherm in temperate and tropical climates, Int. J. Satellite commun, Vol. 8, p 187-196.

Ajewole, M.O (2003): 'Scattering and attenuation of centimeter and millimeter radio signals by tropical rain' PhD Thesis, Federal University of Technology Akure, Nigeria.

Ajewole, M.O (2003): Bistatic interference due to tropical rainfall types: a comparison of rain-cell models, Atti Della Fondazione Giorgio Ronchi, Vol.58, No.1,p 129-141.

Ajewole, M.O, Kolawole, L.B, and Ajayi, G.O (1999): Evaluation of bistatic intersystem interference due to scattering by hydrometeor on tropical paths, Int. J. satellite commu.Vol.17, p339-356.

Awaka, J. and Oguchi, T. (1982): Bistatic radar reflectivities of pruppacher- and-pitter form raindrops at 34.8GHz, Radio sci. Vol.17, No1, p 269-278.

Capsoni, C.and D'Amico, M. (1997): A physically based, simple prediction method for scattering interference. Radio science, Vol. 32, No2, p 397-407.

Capsoni, C. D'Amico, M, Martellucci,A, Oladano,L and Paraboni,A (1992): A 3D prediction method of scattering interference complete versus pencil beam approximation, Proc. URSI Comm. F. open, symp. On wave propagation and remote sensing, Ravenscar, England, p 8-11.

Capsoni, C.Fedi, F, Magistroni, C, Paraboni, A, and Pawlina, A. (1987): Data and theory for a new model of the horizontal structure of rain cells for propagation applications Radio Sci. Vol. 22, No3, p 395-404.

Commission of the European Communities on Cooperation in the fields of Scientific and Technical research, COST 210: Influence of the atmosphere on interference between radio communication systems at frequencies above 1GHz, Final Rept, EUR 13407EN, Brussels, 1991.

Crane, R. (1974): Bistatic scatter from rain, IEEE Trans. Ant. And Propag; A&P 22, No2. p 312-320

International Telecommunication Union- and Radio communication ITU-R (1999): Characteristics of precipitation for propagation modeling. Geneva p 837-2

ITU-R (1997): Surface density and total columnar content, Geneva. P 836-1

Marshall, J.S and Palmer, W.M.K (1948): The distribution of raindrops with size. J. Meteorol; Vol. 5, p 165-166.

McCarthy, D.K, Allinut, J.E, Salazar, W.E, Omeatar, E.C, Owolabi, B.R, Oladiran, T, Ojeba, E.B, Ajayi, G.O, Raji, T.I and Ziks.C (1994a): Results of 11.6GHz radiometric experiment in Nigeria. Second year Electron letter, Vol.30, No.17 p 1452-1453.

McCarthy, D.K, Allinut, J.E, Salazar, W.E, Wanmi, F, Tehinda, M, Ndinayi, T.D.G and Zaks, c. (1994b): Results of 11.6GHz radiometric experiment in Cameroon. Second year Electron letter, Vol 30, No17, p 1449-1450.

McCarthy, D.K, Allinut, J.E, Salazar, W.E, Sitati, R.W, Okoth, M, Mutungii, M.J, Odhiambo, C.D and Zaks, C (1994c): Results of 11.6GHz radiometric experiment in Kenya. Second year Electron, letter vol.30, No. 17 p1450-1451.

Medeiros Filho, F.C, Cole, R.S and Serma, A.O (1986): Millimeter wave rain induced attenuation: theory and experiment IEE proc. Vol. 133 pt. H, No.4, p 308-314

Mismie, P. and Waldteufel, P: (1980): A model for attenuation by precipitation on a microwave earth- space link. Radio Sci. Vol.15, p 655-665.

Olsen, R.L. (1993); Interference due to hydrometeor scatter on satellite communication links. Proc. IEEE Vol. 81, No.6, p 914-922.

Ray, P.S. (1972): Broadband complex refractive indices of ice and water, Applied optics. Vol.11, No.8,p 1836-1844.

Sitorus, S.P and Glover, I.A. (2000): Rapid bistatic scatter calculations using non-orthogonal function expansion of reflectivity profiles, Int. J. satellite. Commu. Vol.18, p 207-218.

Thurai, M. (1994): Climatic parameters required for the prediction of interference due to precipitation scatter.